# Stress analysis on the inductor parts during electromagnetic pulse forming and welding processes using numerical simulations

T. Sapanathan[1], K. Yang[1], R. N. Raoelison[1, 2], D. Jouaffre[3], N. Buiron[1], M. Rachik[1]

[1] Sorbonne universités, Université de technologie de Compiègne, laboratoire Roberval, France
[2] Université de Bourgogne Franche Comté, Université de Technologie de Belfort Montbéliard, France
[3] PFT INNOVALTECH, Rond-point Frédéric Joliot-Curie, Saint-Quentin, France

L'allocation post-doctorale relative au projet COILTIM est cofinancée dans le cadre du Fonds européen de développement économique et régional (FEDER) 2014/2020.

# Project COILTIM: An overview

- Producing efficient welding for similar / dissimilar metal pairs
- Joint quality analysis with process parameters
- Investigations of Interfacial characteristics
- Modeling and simulation of the MPF/MPW
- Development of processing tools and feasibility study

[MPF/MPW: Magnetic Pulse Forming / Magnetic Pulse Welding]

UNION EUROPEENNE

L'allocation post-doctorale relative au projet COILTIM est cofinancée dans le cadre du Fonds européen de développement économique et régional (FEDER) 2014/2020.

PICARDIE LA RÉGION

l'Europe s'engage en Picardie avec le FEDER

# Presentation outline

1. Stresses on a **helix coil** during ring expansion test
2. Stresses on the **flat coil** during forming tests
3. Stresses on the **fieldshapers** in a one turn coil

[EM: Electromagnetic; EMPF: Magnetic Pulse Forming; EMPW: Magnetic Pulse Welding ]

# Model specifications

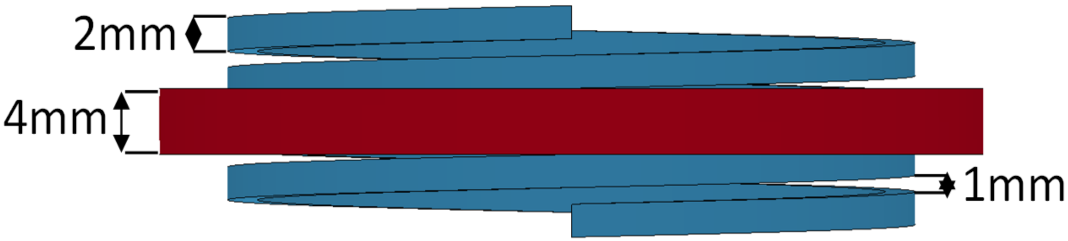


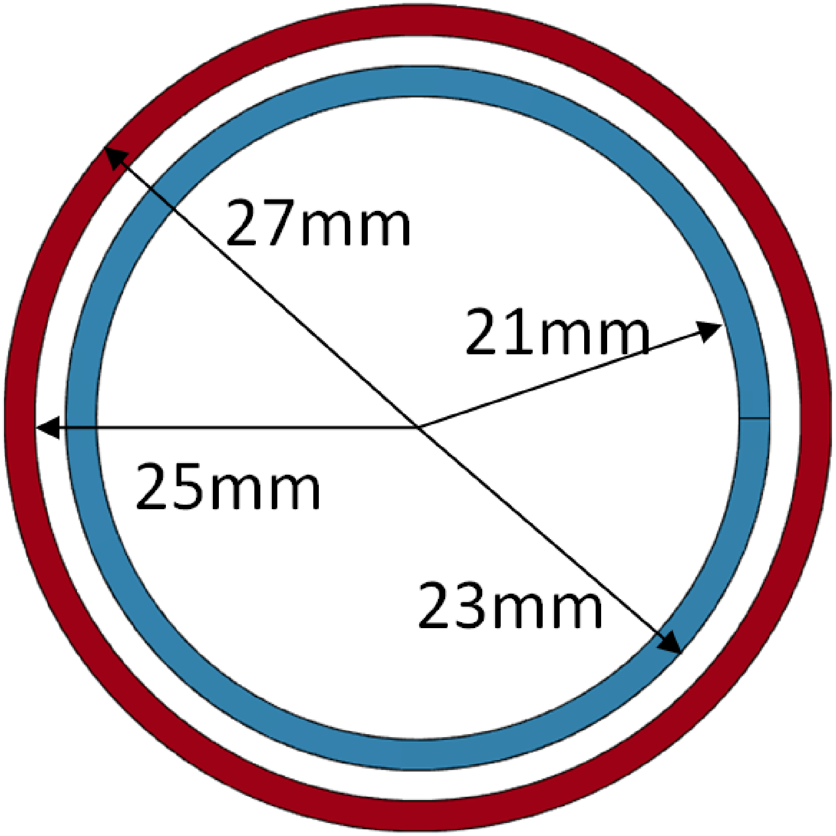


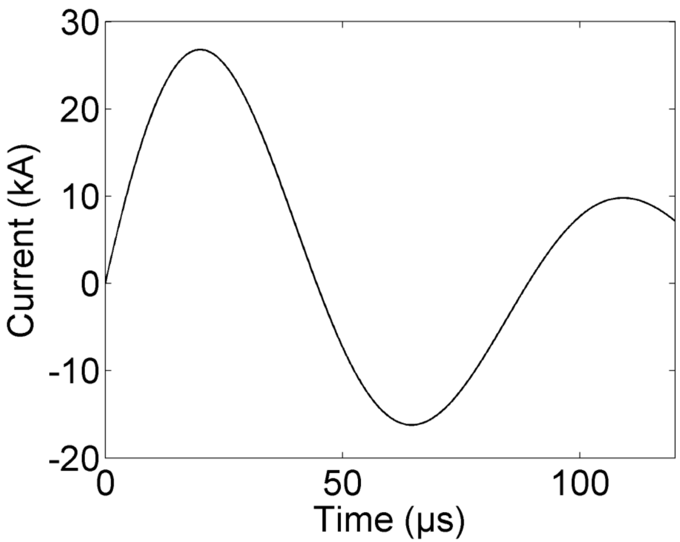


Input current

## Helix coil steel properties

| Density ($g/mm^3$) | Young's Modulus | Electrical conductivity |
|---|---|---|
| 7.9 | 210 GPa | 18.5 IACS% |

# Three different boundary conditions used for a helix coil geometry in a cylindrical coordinate system

## Case 1

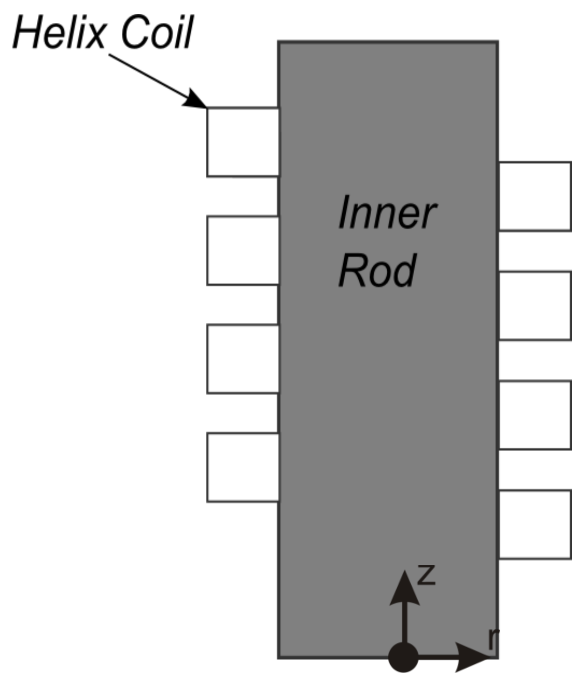


Coil can move towards + r and $\pm$ z directions

## Case 2

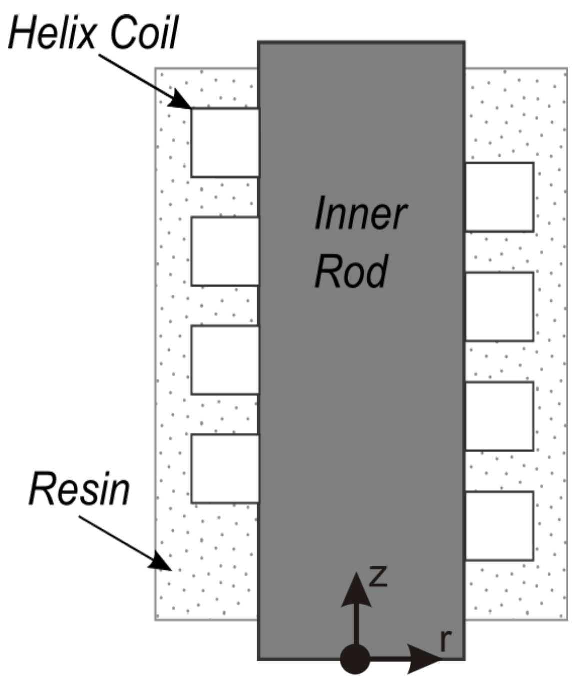


All the coil surfaces are fixed

## Case 3

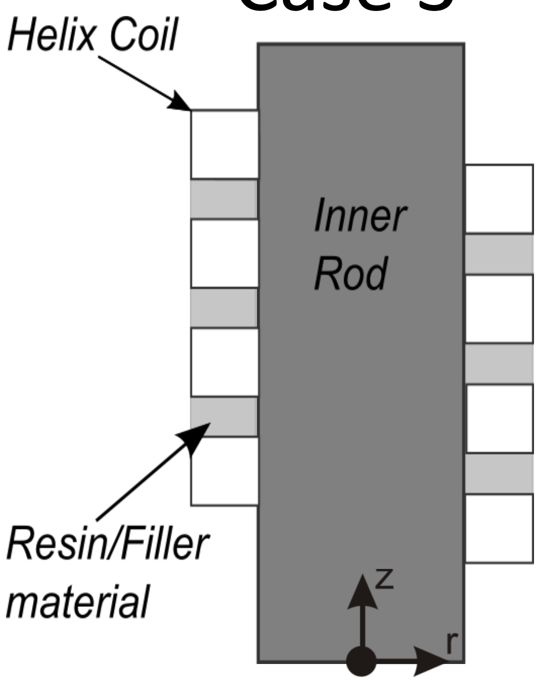


Coil can only move towards +r direction

# von Mises stresses on the coil

Case 1: Maximum stress 1954 MPa at 38 μs (when calculation was terminated due to large deformation)

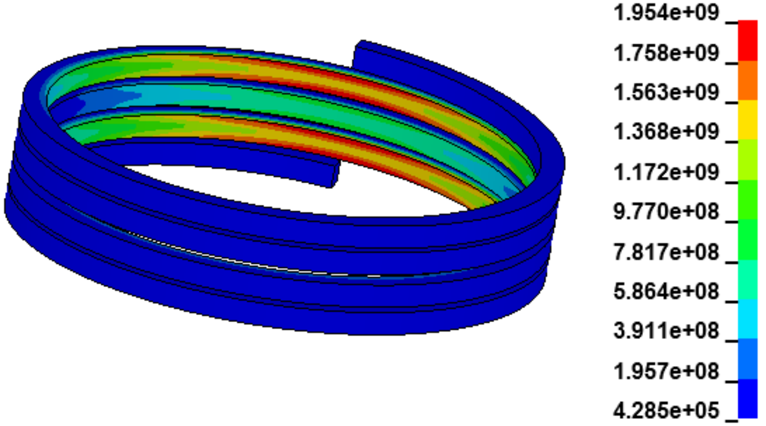


Case 2: Maximum stress 10.3 MPa at 22 μs

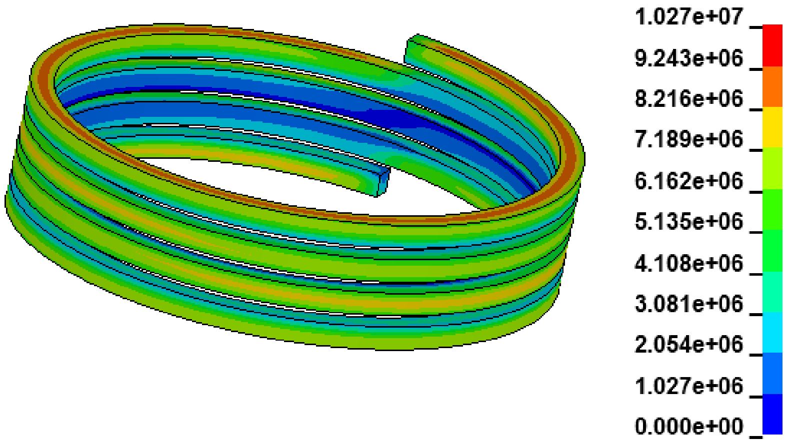


Case 3: Maximum stress 20.1MPa at 19 μs

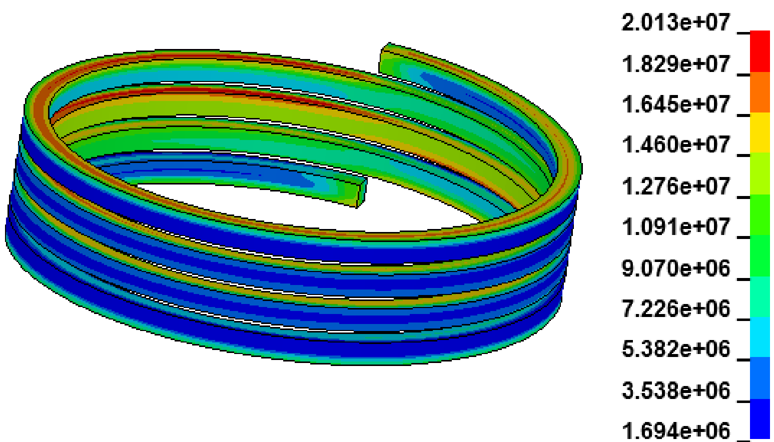

# Component of stresses on the coil

- In Case 1, Shear stress is significantly higher than the normal stresses.

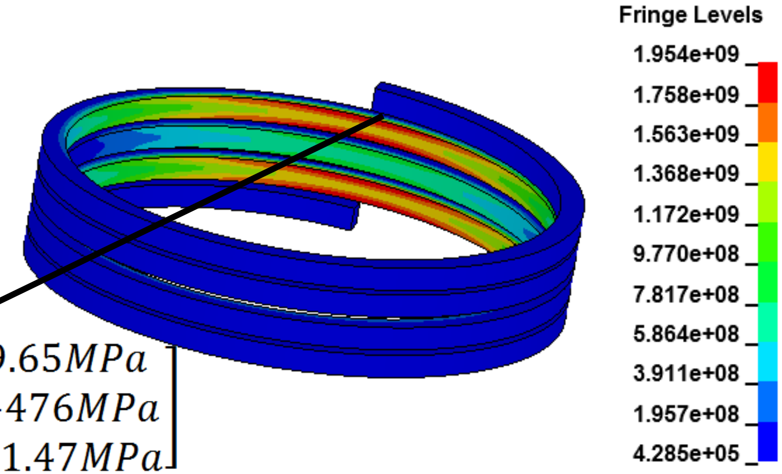


Stress: $$\begin{bmatrix} -24.7MPa & 1020MPa & 9.65MPa \\ & 5.15MPa & -476MPa \\ & & -1.47MPa \end{bmatrix}$$

- Maximum stress appears on same region of coil for Cases 2 and 3.

- Shear stresses are negligible in comparison with the normal stresses.

- Outer surfaces bear higher stress than that of the inner surfaces in Case 2.

- Case 3 shows the reverse behavior and the inner surfaces bear higher stress comparing to the outer ones.

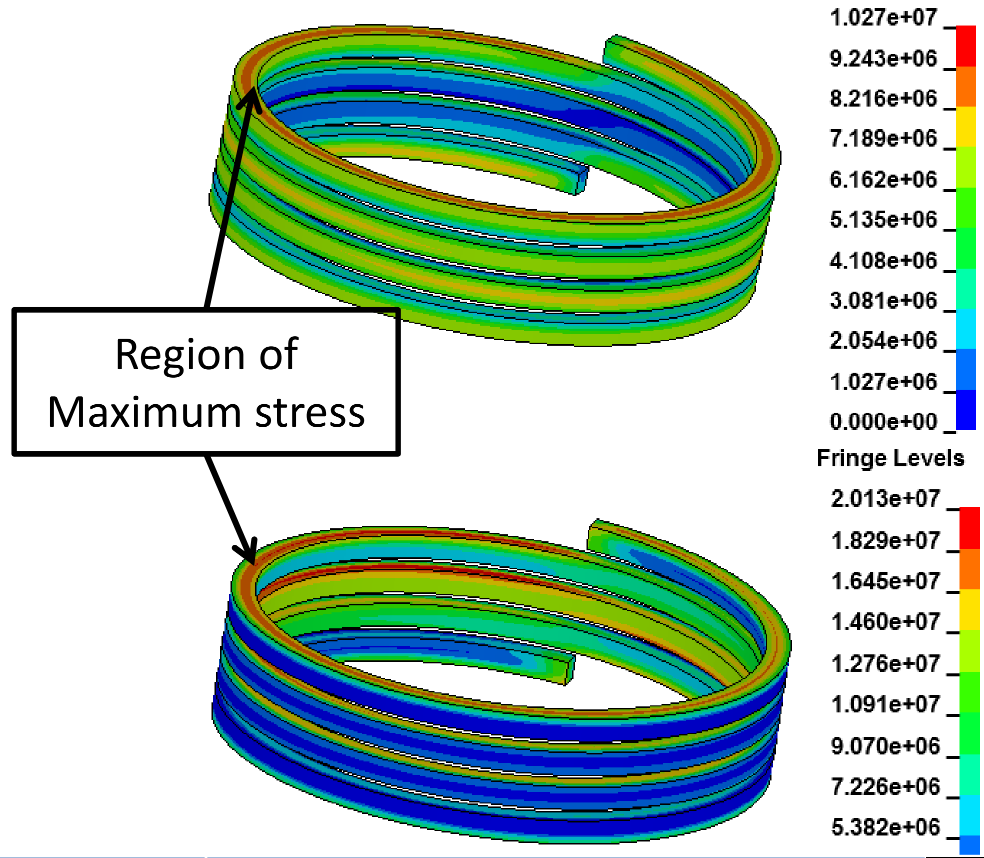

# An industrial forming case study

## Assembly and parts of simulations

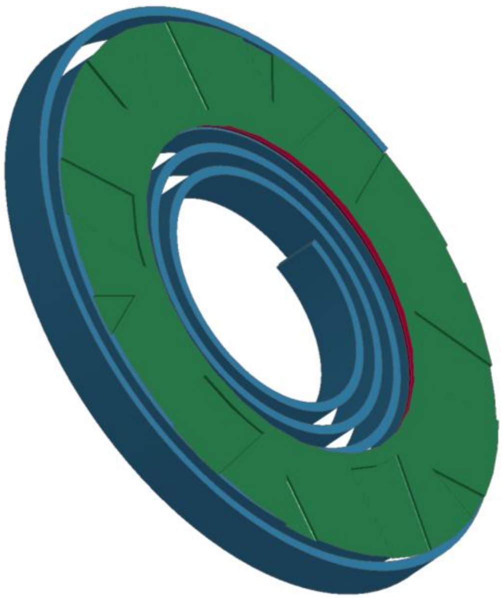

Assembled Geometry

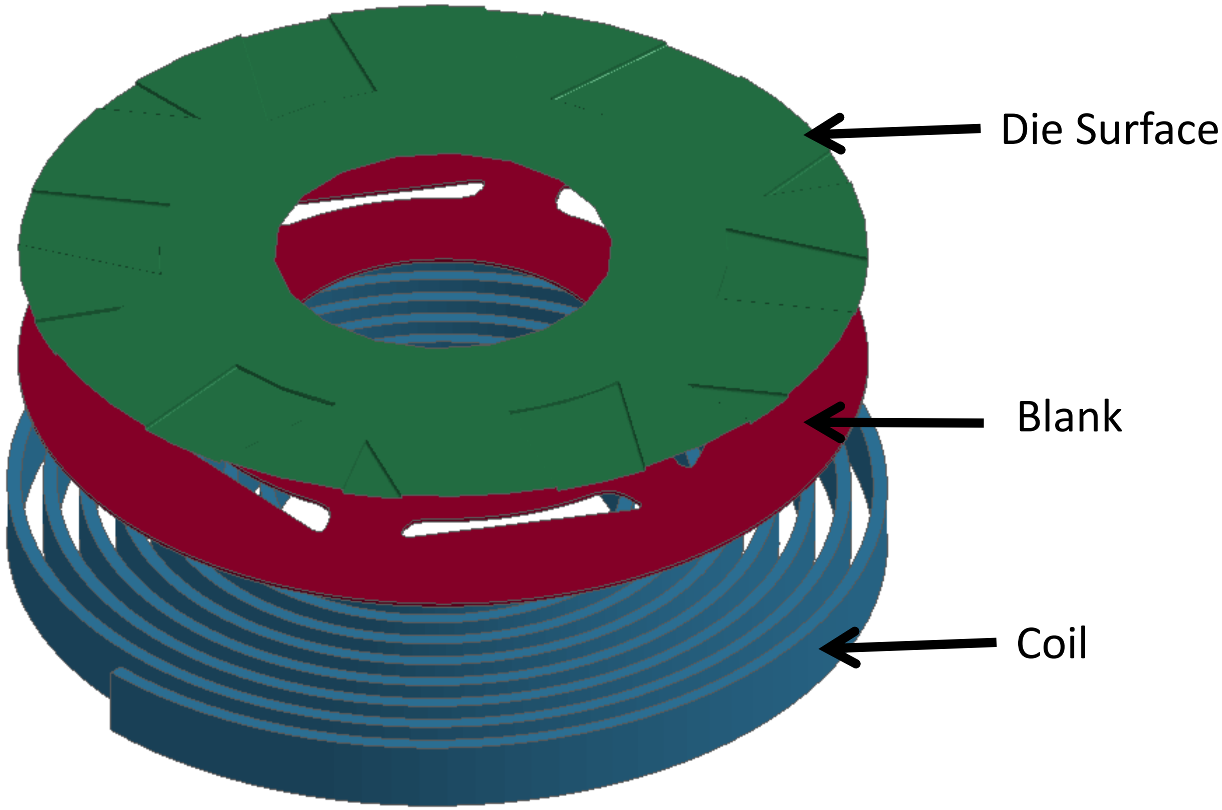


Preliminary model assembly: Gap between the coil and blank is set as 1mm
Gap between the blank and die is set as 2mm

# Material parameters

Mechanical and electromagnetic properties of materials used in this model

| Material | Part | ρ (g/mm³) | Young's modulus (GPa) | Poison ratio | Electrical conductivity (S/m) |
|---|---|---|---|---|---|
| Hard Steel | Plate | 7.9 | 210 | 0.29 | $5.8 \times 10^6$ |
| Copper alloy | Coil | Rigid | | | $4.06 \times 10^7$ |
| Steel | Die | Rigid | | | - |

Simplified Johnson-Cook model used in LS-Dyna simulation

$$\bar{\sigma} = (A + B\bar{\varepsilon}^n)\left[1 + C ln\left(\frac{\dot{\varepsilon}}{\dot{\varepsilon}_0}\right)\right]$$

| Material and part | A | B | n | C | m |
|---|---|---|---|---|---|
| Hardened Steel plate | 960 | 824 | 0.51 | 0.017 | 1 |

Stresses on the coils are calculated using elastic properties of the materials

# von Mises stresses at 36μs

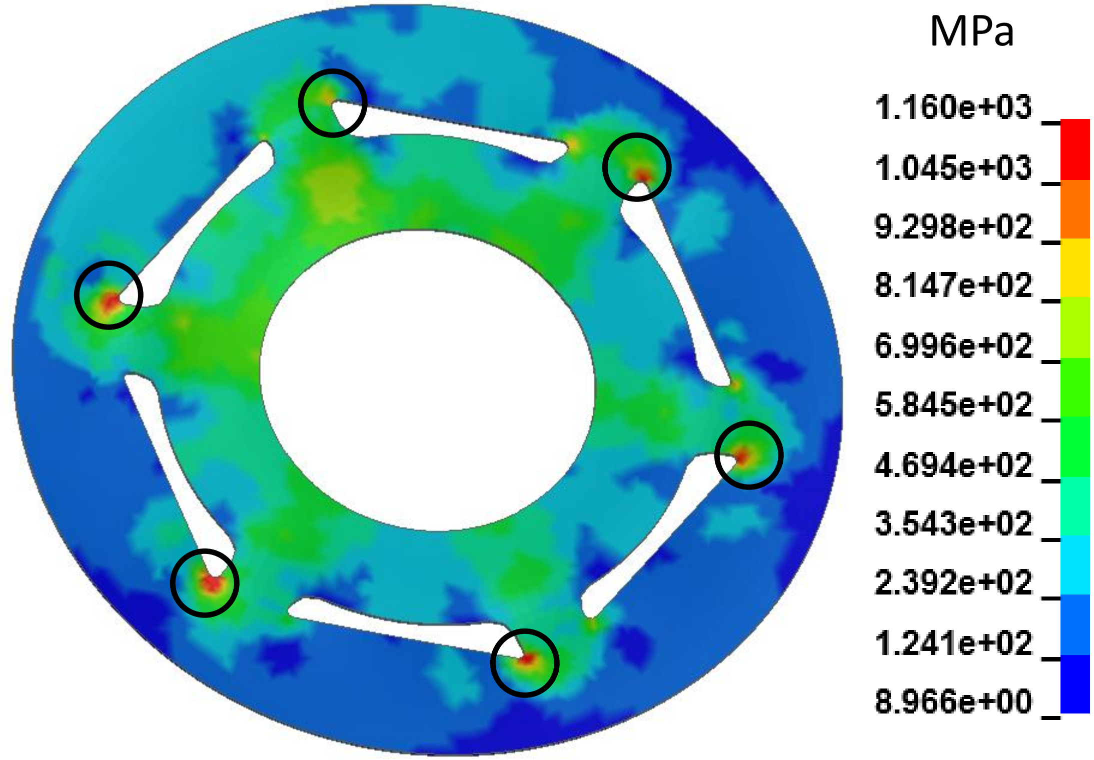


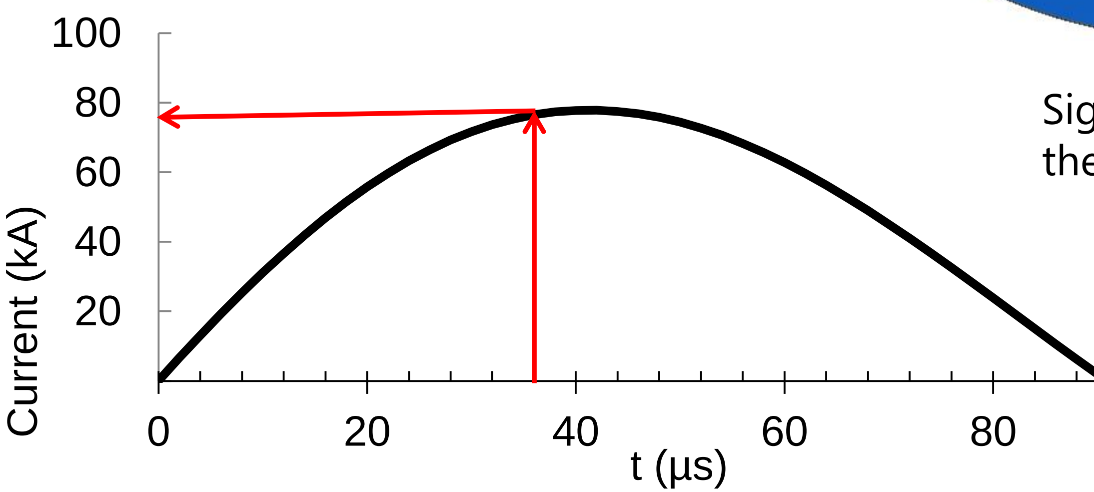


Significant stress concentration occurs at the corners due to localised current flow

# Plastic Strain at various time steps for a flat plate without featured holes

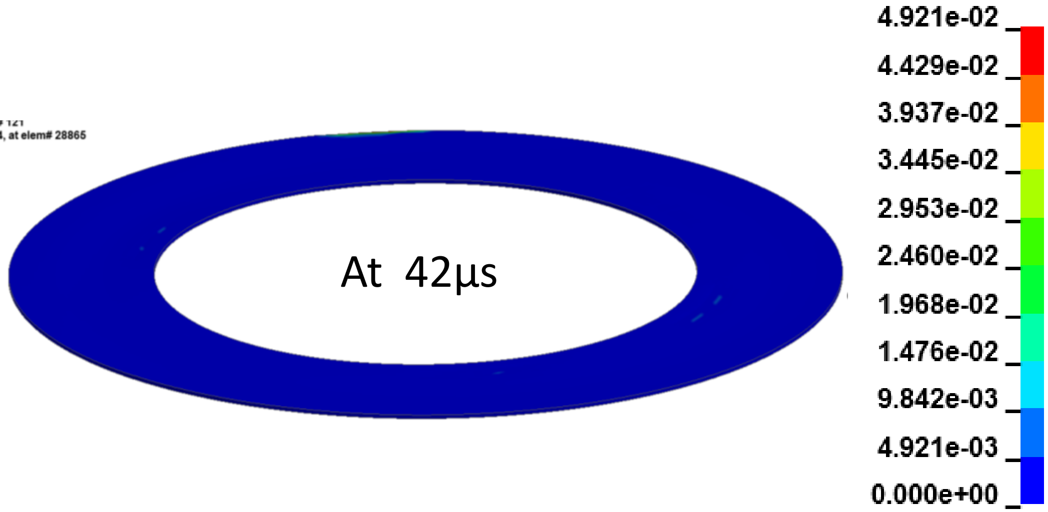


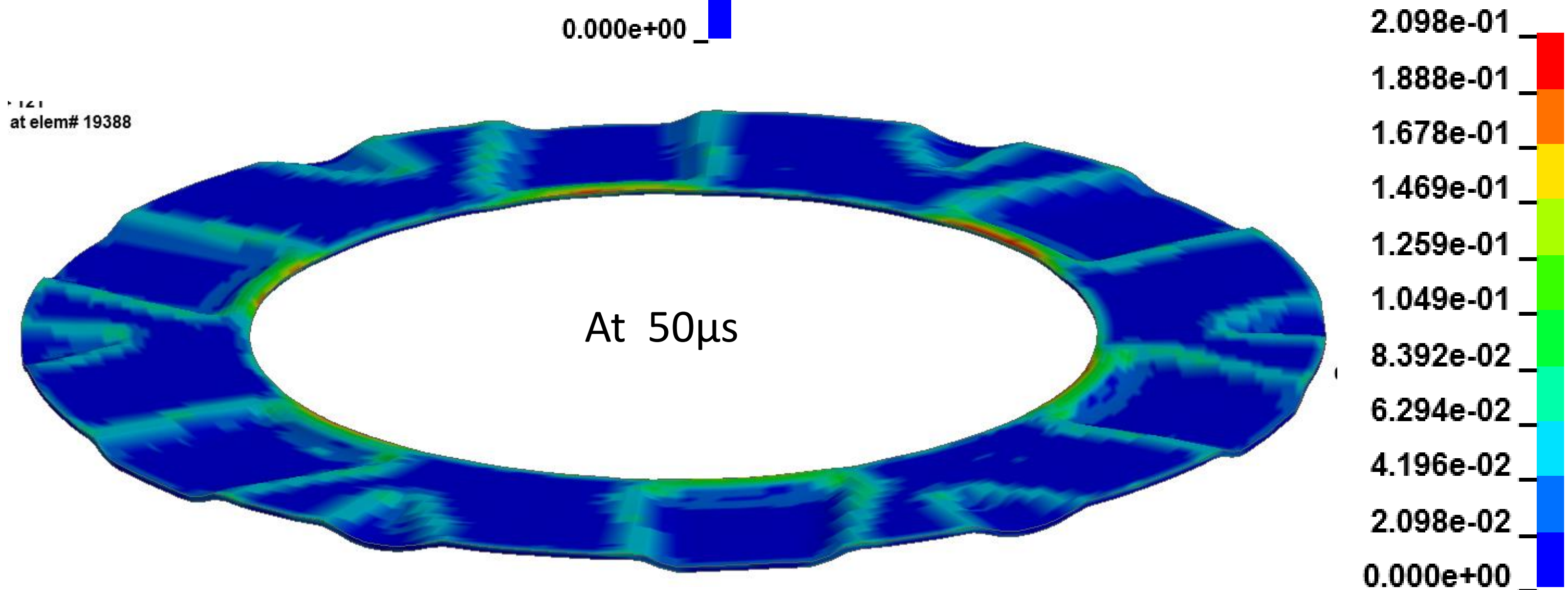

# Plastic strain at 68µs for the flat plate without featured holes

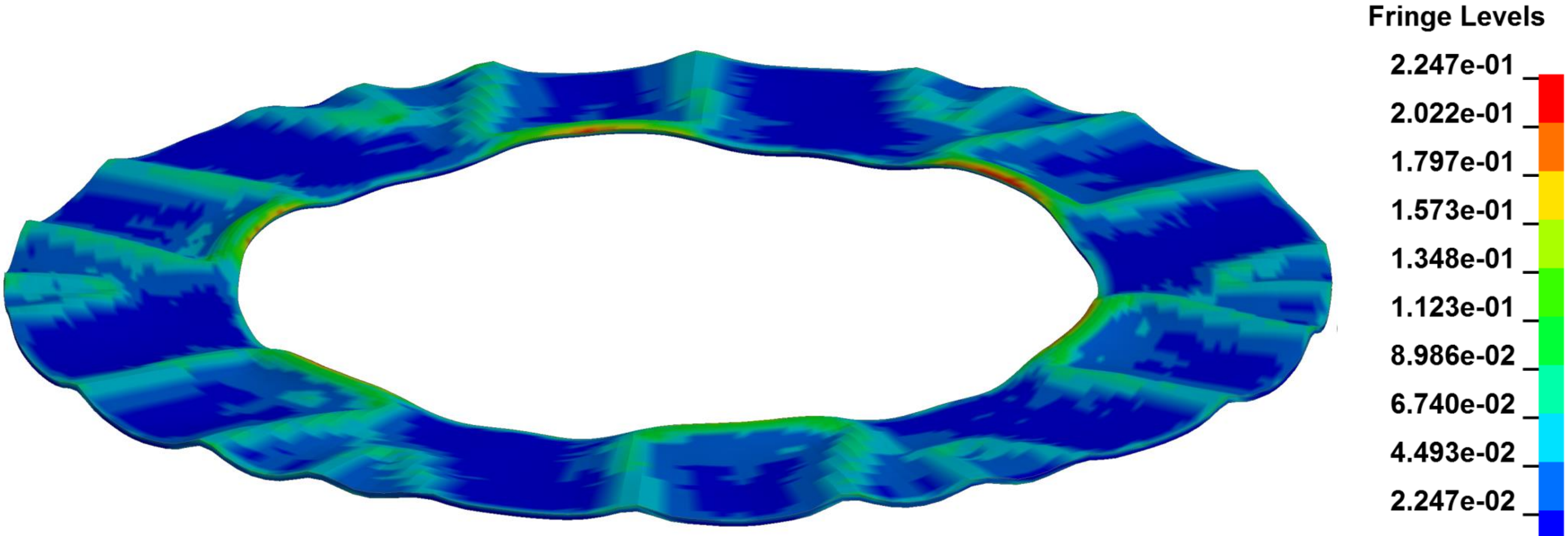


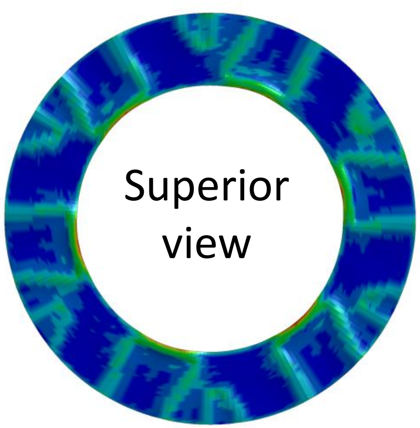


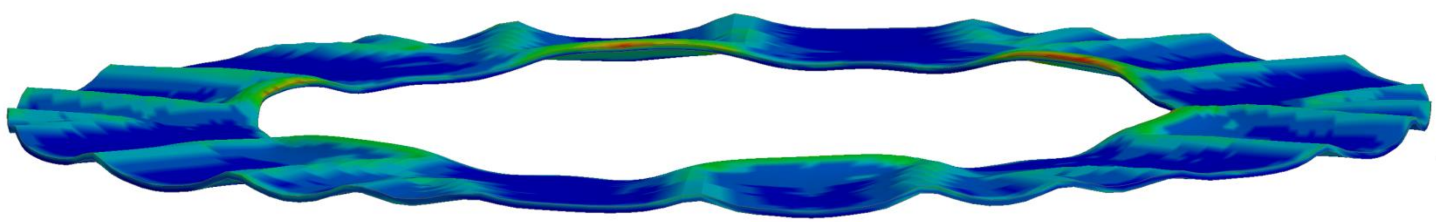

# von Mises Stress at the peak current time step (42 µs) without featured holes

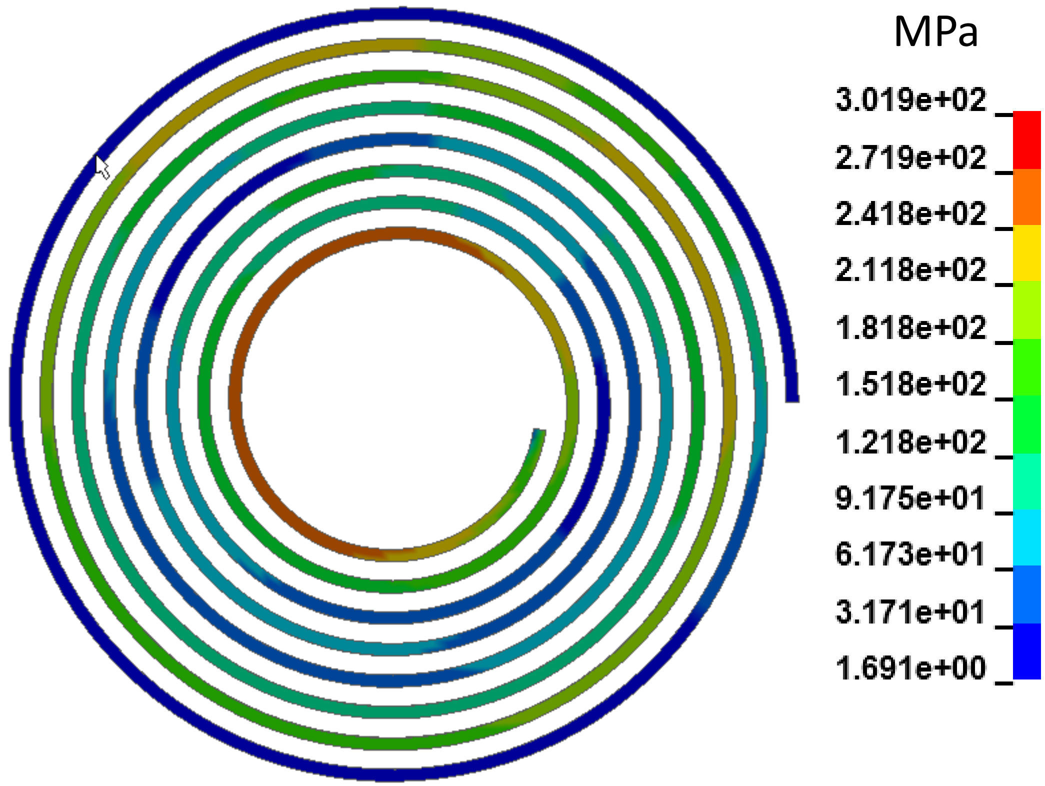


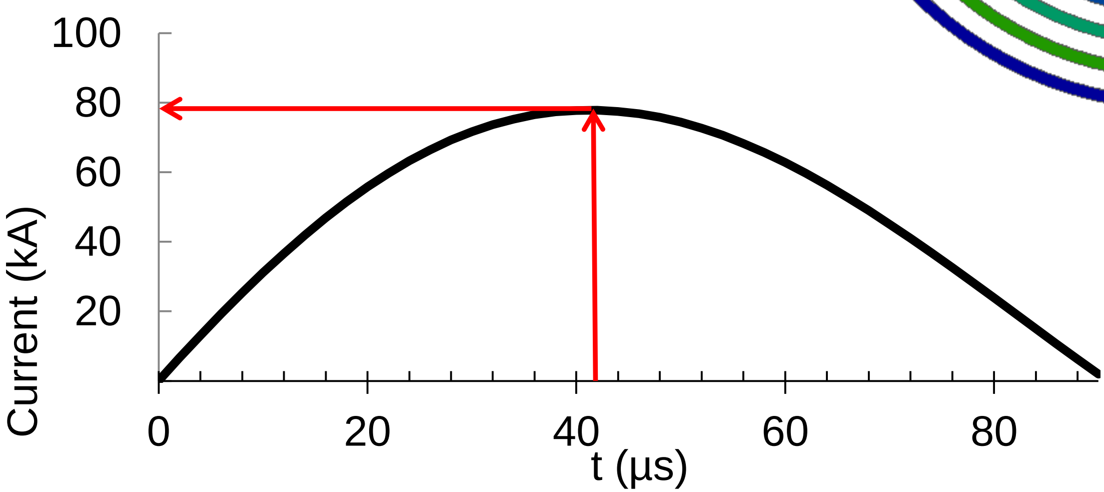

# Maximum von Mises Stress on the coil at 68 μs without featured holes

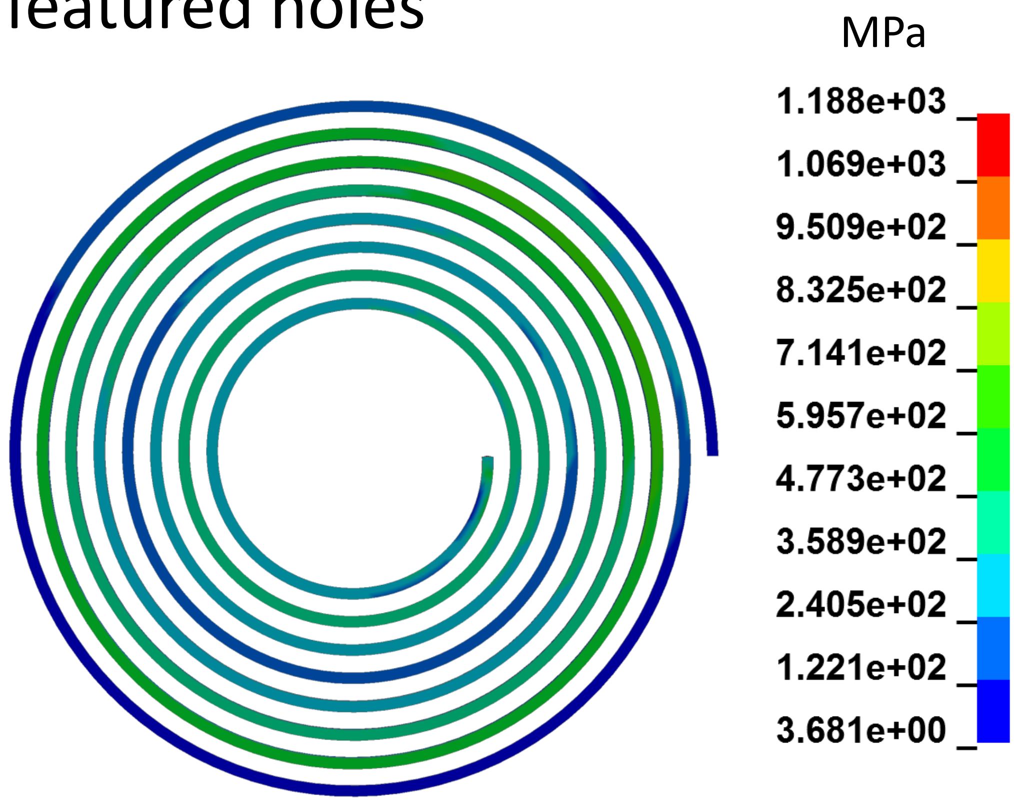


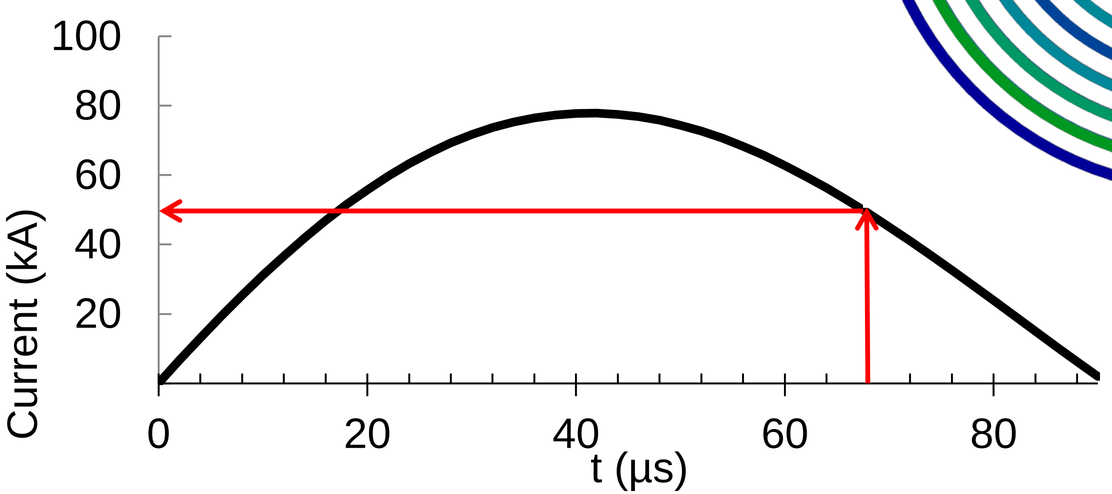

# Limitations in maximum allowable current

1. The mechanical force is very high on the coil, same as the one acting on the workpiece

- Research studies shows various reinforcement techniques
- The best choice could be Zylon fibre

2. Temperature increase of the coil

- it also depends on the processing time
- Material
- Using an additional sub electric circuit was used to minimise the thermal effect

Qiu et al., 2012, Design and Experiments of a High Field Electromagnetic Forming System

Cao et al., 2015, Analysis and reduction of coil temperature rise in electromagnetic forming

# Forming with driving plate
## example (1): DP 780 steel

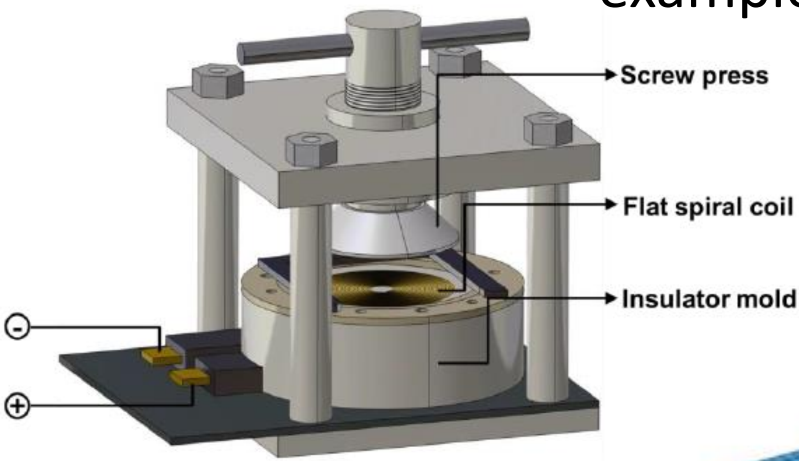


Forming setup

Assembly Order

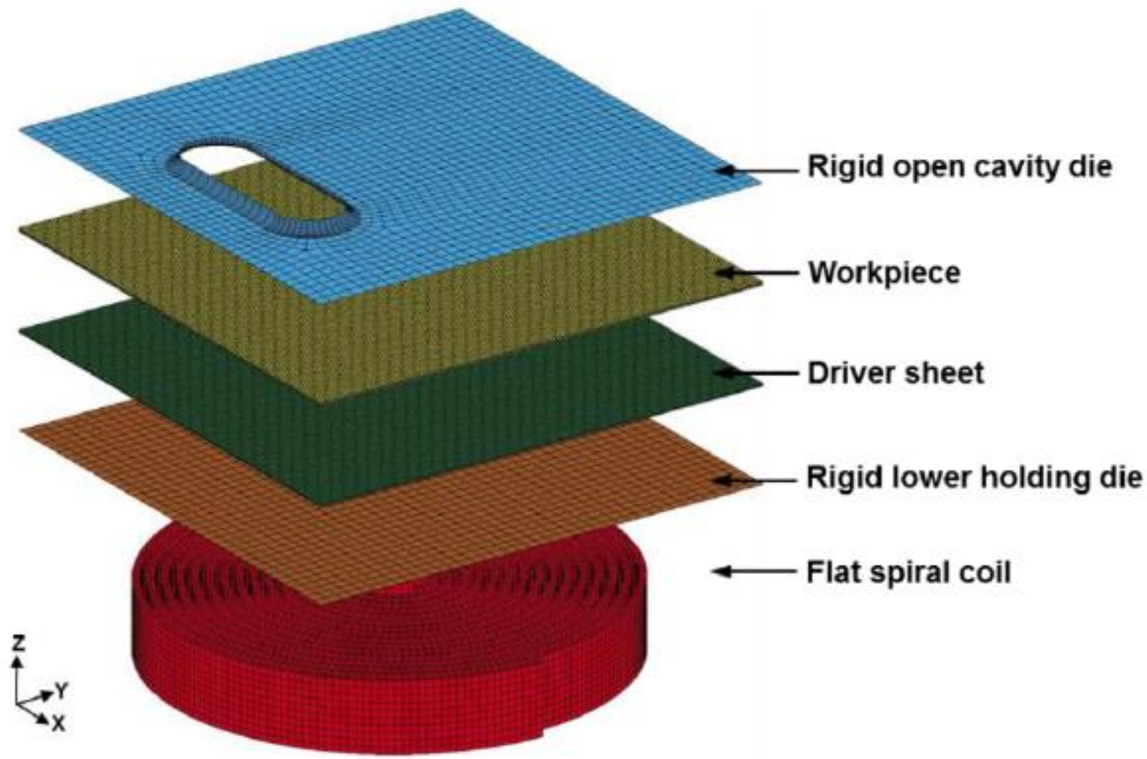


H. Park et al., "Effect of an aluminum driver sheet on the electromagnetic forming of DP780 steel sheet," *Journal of Materials Processing Technology,* vol. 235, 2016

# Experimental and numerical results for the DP 780 steel

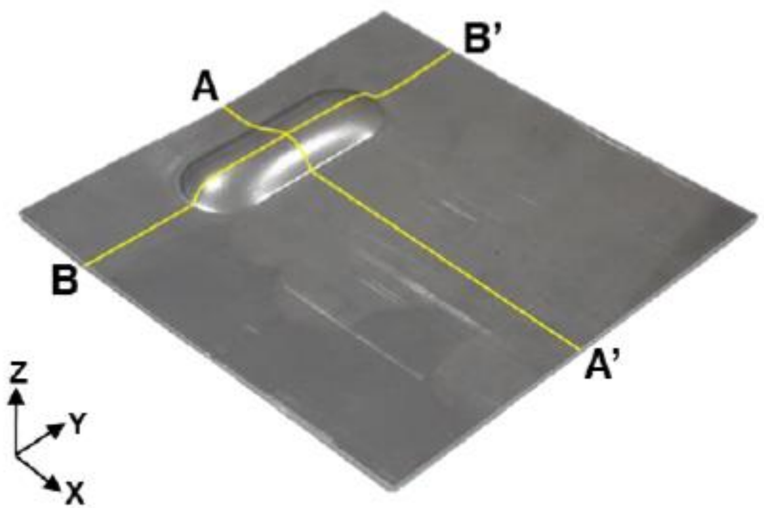


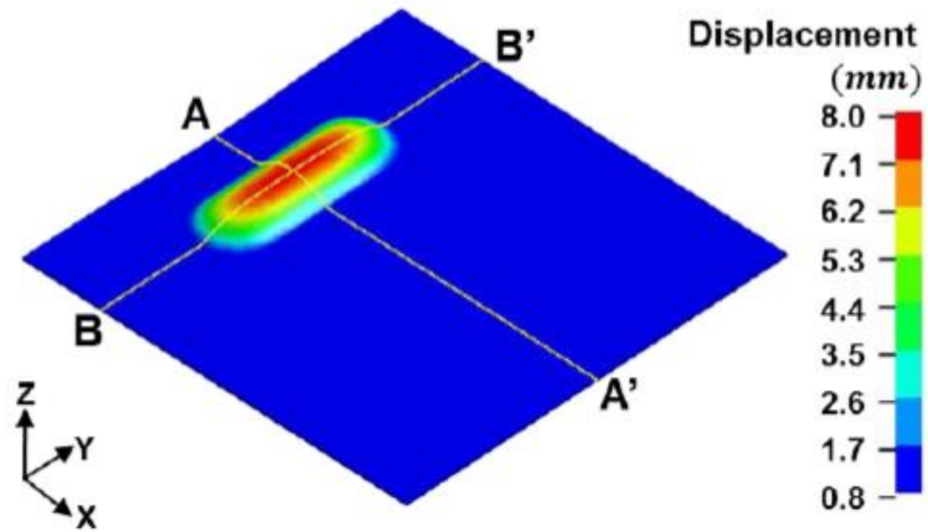


H. Park et al., "Effect of an aluminum driver sheet on the electromagnetic forming of DP780 steel sheet," *Journal of Materials Processing Technology,* vol. 235, 2016

# Example 2: for stainless steel and cold roll carbon steel

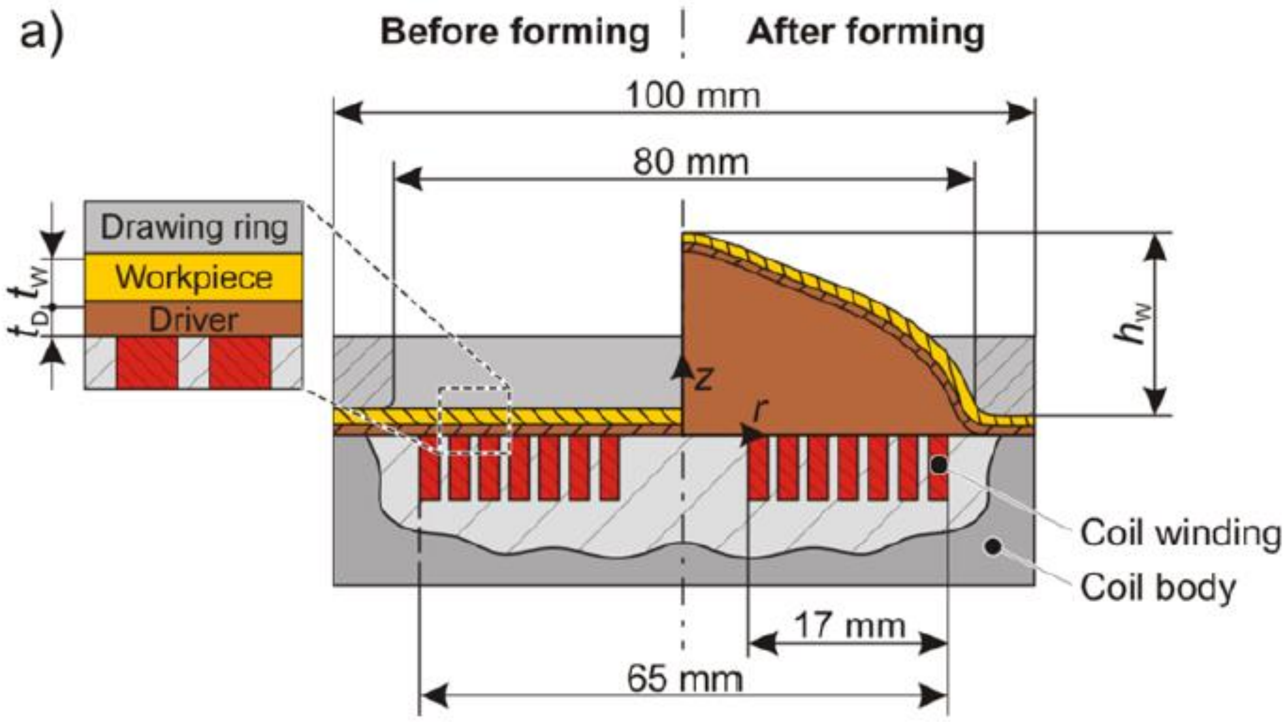


Free forming experimental setup


Driver plate and workpiece after the process

S. Gies, C. Weddeling, and A. Tekkaya, "Experimental Investigations on the Optimum Driver Configuration for Electromagnetic Sheet Metal Forming," 2014

# Typical driving plates and their geometries from Literature

| Workpiece | | Driver | | $t_D/\sigma_S$ |
|---|---|---|---|---|
| Material | Thickness $t_W$ | Material | Thickness $t_D$ | |
| DC04 | 0.80 mm | Copper | 0.65 mm | 1.0 |
| Titanium | 0.50 mm | Copper | 0.65 mm | 1.0 |
| DP600 | 0.70 mm | Copper | 0.60 mm | 0.90 |
| Ti-6AL-4V | 0.50 mm | CU-DHP | 0.50 mm | 0.82 |
| X5-CrNi18-10 | 0.15 mm | EN AW-1050 | 0.30 mm | 0.73 |
| X5Cr-Ni-Mo17-12-2 | 0.25 mm | Copper | 0.10 mm | 0.22 |
| X12CrMn-NiN17-7-5 | 0.08 mm | Copper | 0.15 mm | n/a |
| Titanium | 0.08 mm | Copper | 0.15 mm | n/a |
| Carbon steels | 0.15 – 0.3 mm | EN AW-6111 | 1.0 mm | n/a |
| AZ31B-O (Mg) | 0.55 mm | Aluminum | n/a | n/a |
| Titanium CP-1 | 0.50 mm | Aluminum | n/a | n/a |

$\sigma_S$ : Skin depth

S. Gies, C. Weddeling, and A. Tekkaya, "Experimental Investigations on the Optimum Driver Configuration for Electromagnetic Sheet Metal Forming," 2014

# Driver plate with top die and bottom die

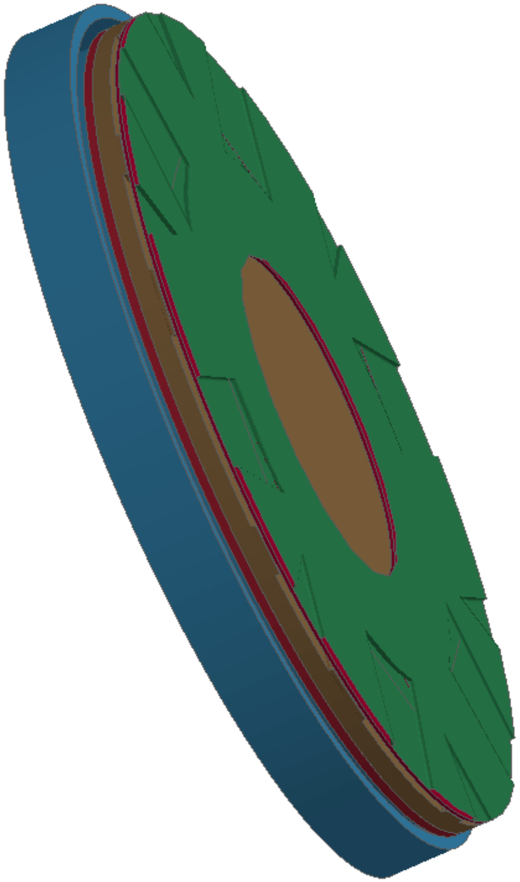

Assembled Geometry

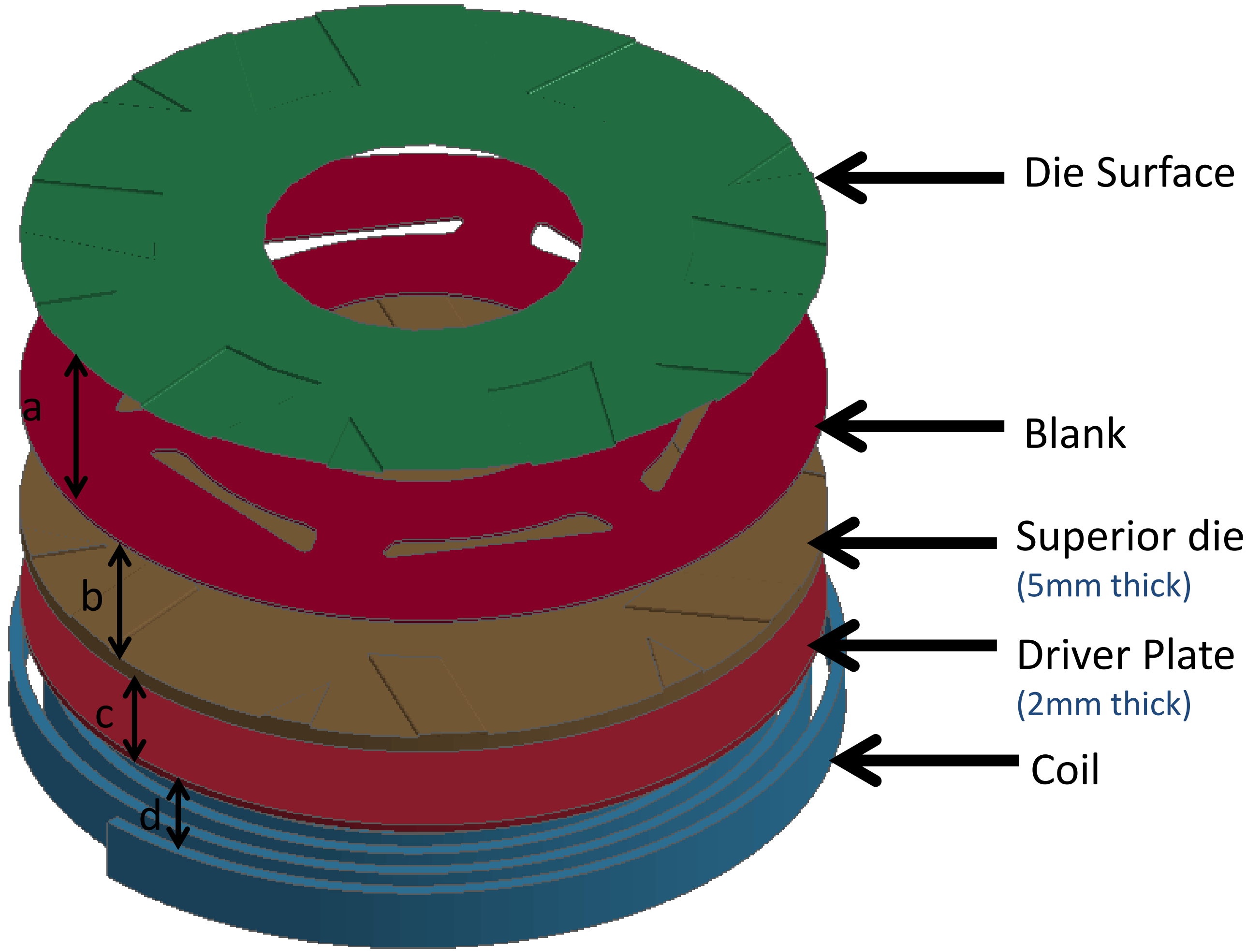


| Gap | a | b | c | d |
|---|---|---|---|---|
| 1st Assembly distance (mm) | 0.01 | 0.19 | 0.0 | 1.0 |

# Comparison of maximum von Mises stresses on the coil with and without the driver plate

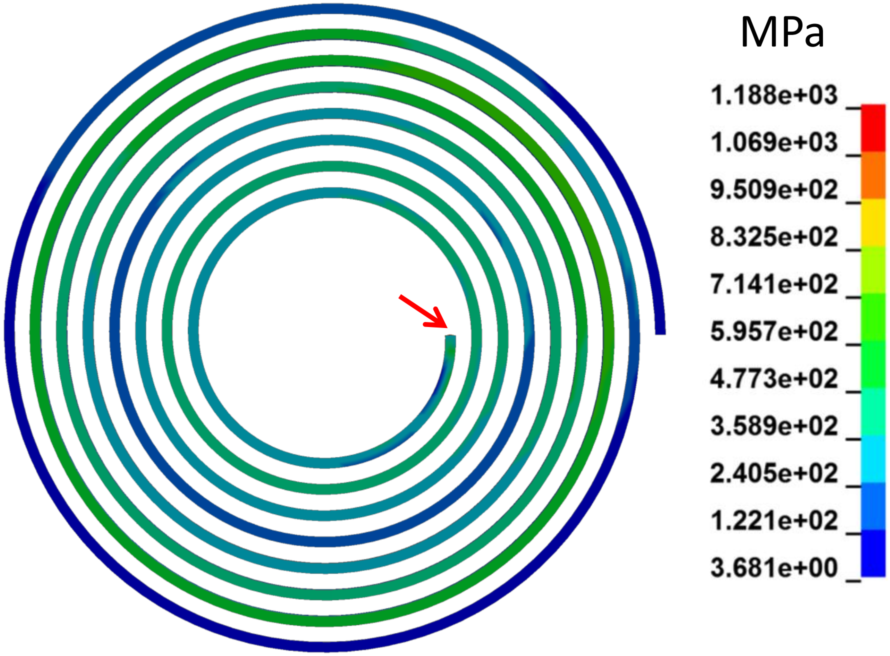


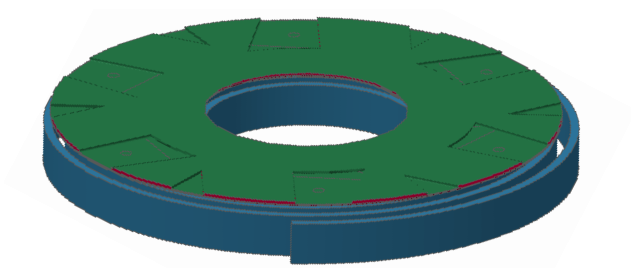

Simple assembly with a plate without featured holes

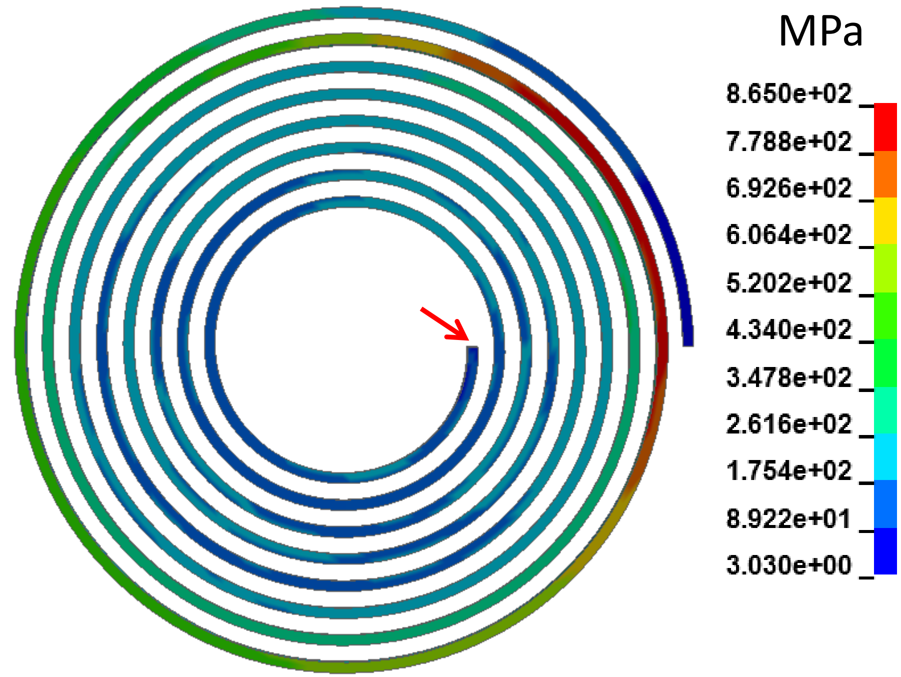


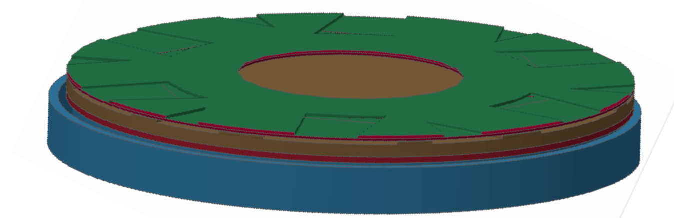

With driver plate assembly

- This difference mainly  occurs due to various tools and the boundary conditions
- Appropriate reinforcement can help to lower the stresses
- Appropriate boundary conditions should be used to improve the accuracy of the models

# von Mises stresses on the coil with the driver plate

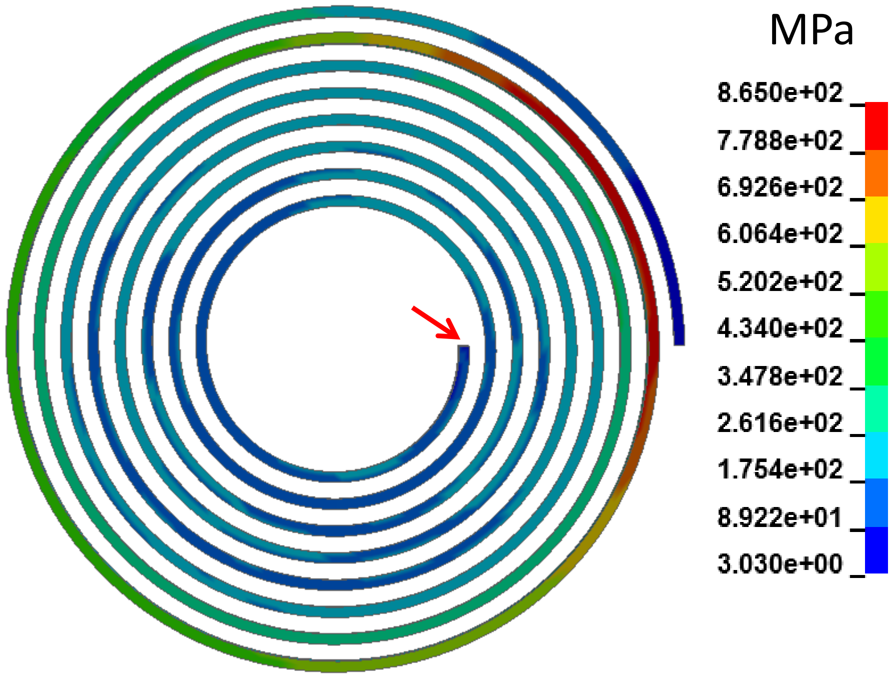


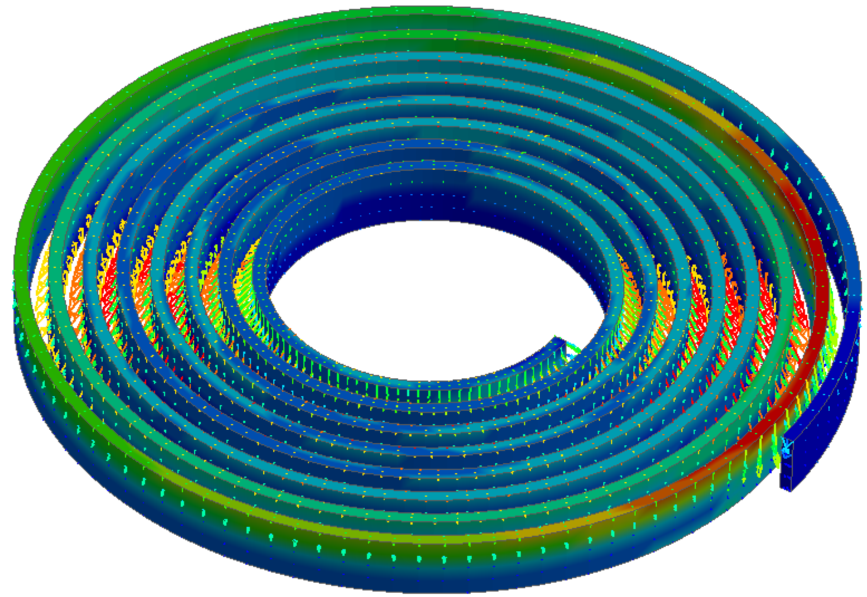

Von Mises stresses indicated by the colour
(Lorentz force vectors are overlaid)

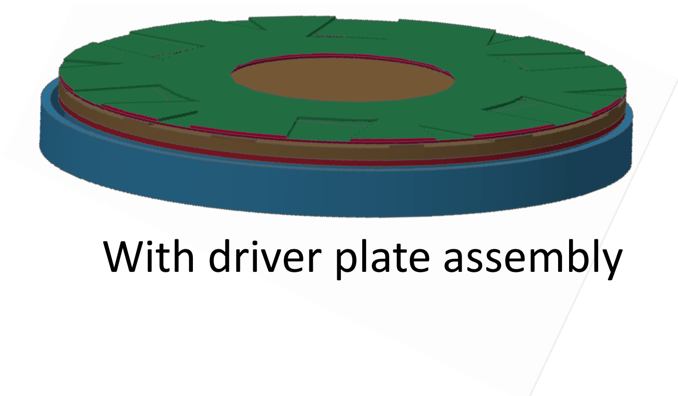

With driver plate assembly

# Single turn coil with field shaper model

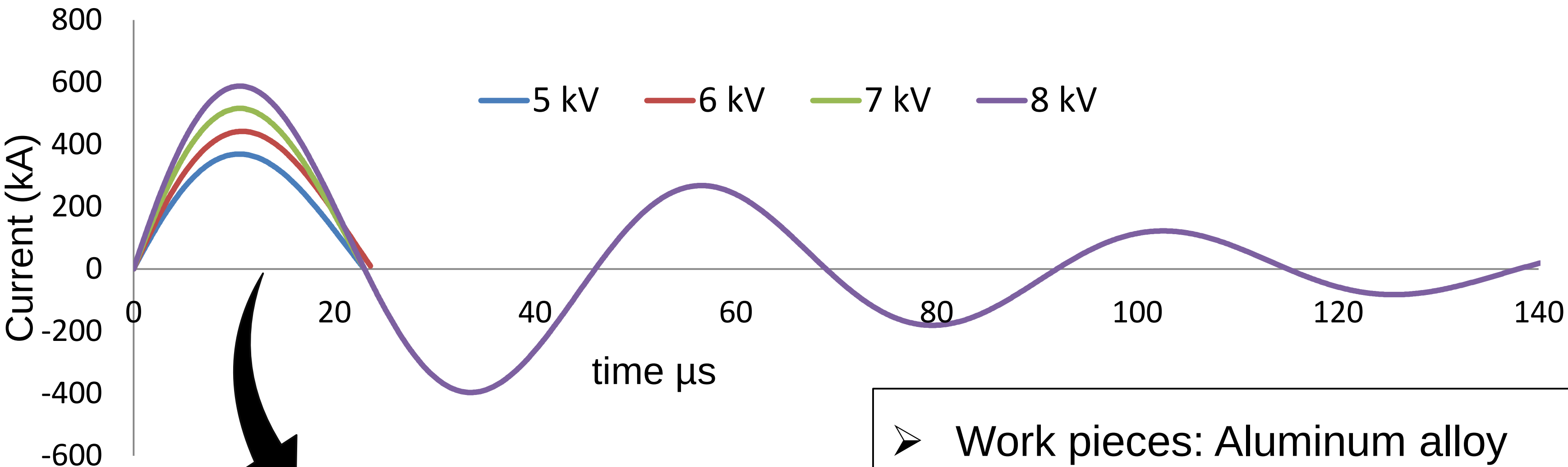


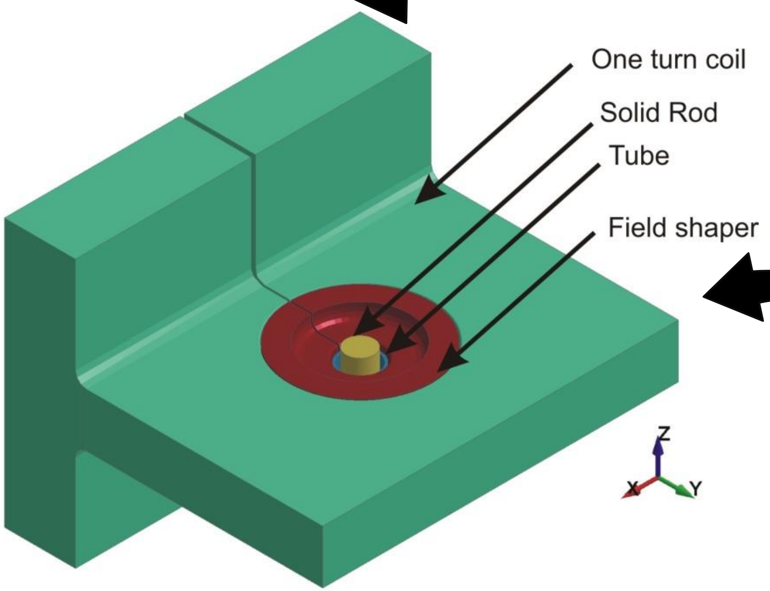


- Work pieces: Aluminum alloy
- Coil: Copper alloy
- Fieldshaper: Copper alloy / Steel

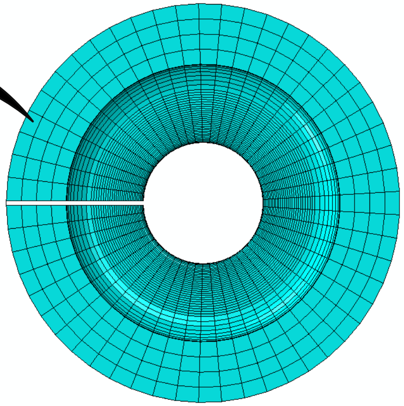

Number of elements in the fieldshaper: 59307

# Coupled electromagnetic-mechanical models

- Mechanical + Electromagnetic contact procedures are used in these models

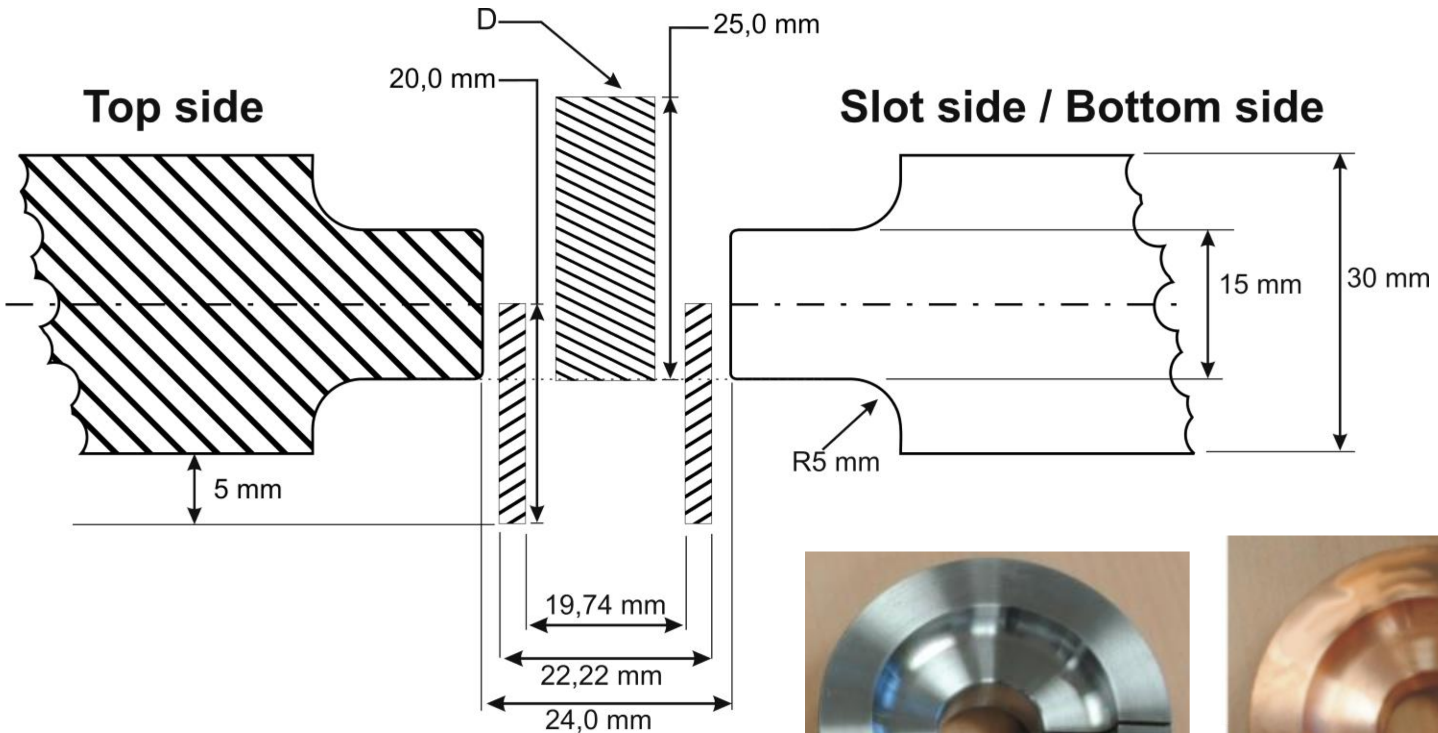


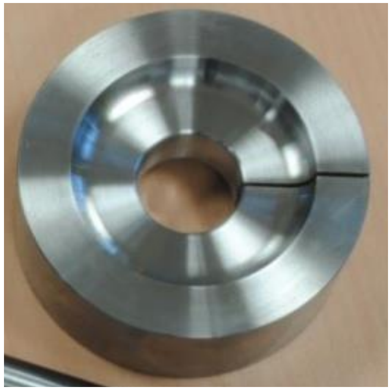

Steel

Copper alloy

# Material parameters

| Material | Components | Density ($kg.m^{-3}$) | Young's modulus (GPa) | Poisson's ratio | Electrical conductivity (IACS%) |
|---|---|---|---|---|---|
| AA2024 – T351 | Tube or Rod | 2700 | 73 | 0.33 | 30% |
| Copper Alloy | Field shaper | 8900 | 140 | 0.29 | 89% or 46% |
| Steel | Field shaper | 7900 | 210 | 0.29 | 10% |
| Copper | Coil | Rigid | | | 46% |

Constitutive model: $$\bar{\sigma} = (A + B\bar{\varepsilon}^n)\left[1 + C ln\left(\frac{\dot{\bar{\varepsilon}}}{\dot{\bar{\varepsilon}}_0}\right)\right]$$

| Johnson-Cook parameters | *A* (MPa) | *B* (MPa) | *C* | *n* |
|---|---|---|---|---|
| Aluminum alloy AA2024-T351 | 352 | 440 | 0.0083 | 0.42 |

# von Mises stress (MPa) on different Fieldshapers at 10 μs

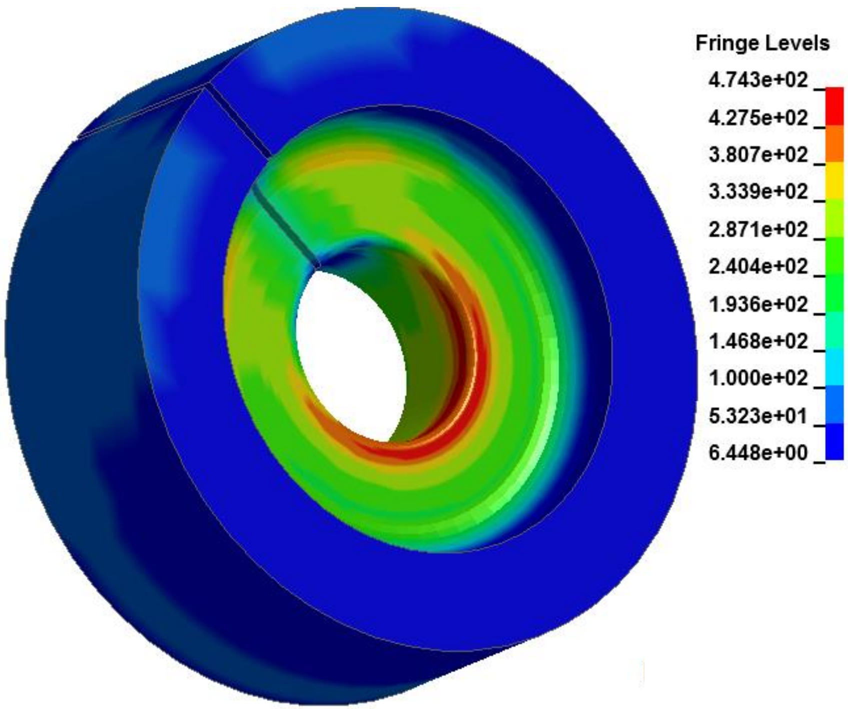


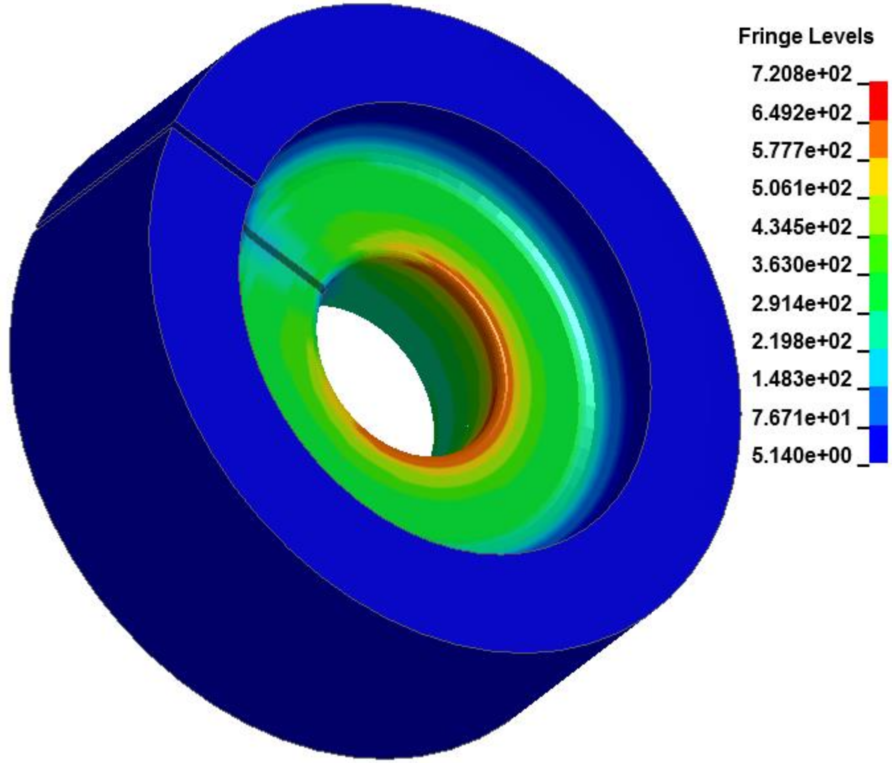


| Steel (10% IACS, Young's Modulus: 210 GPa) (Skin depth 1.39 mm) | Copper alloy (89% IACS, Young's Modulus: 140 GPa) Skin depth 0.46 mm |
|---|---|

- 8kV input Voltage
- 2.5 mm gap between the tube and the rod
- Average mesh size of 0.2 - 0.3mm

# Effect of fieldshaper geometry on stress development

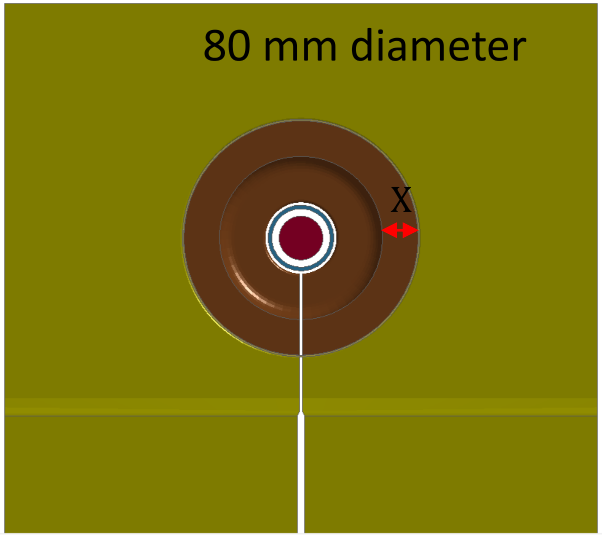


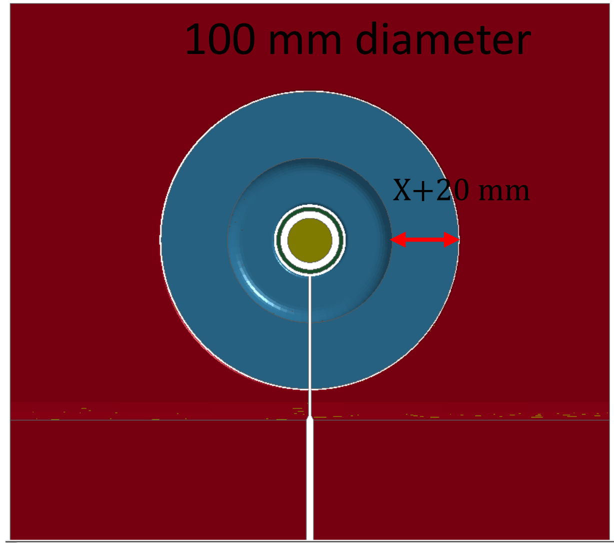


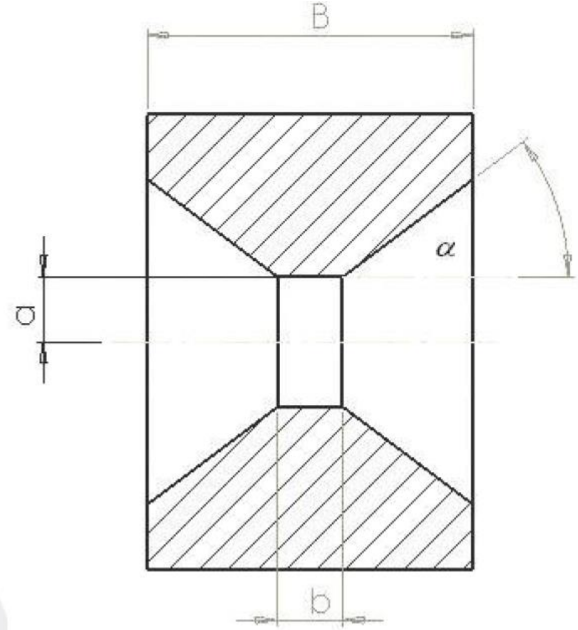


In terms of efficiency

$$C = \frac{B}{b + \frac{a\sin(\alpha)}{1-\cos(\alpha)}}$$

Where:

[B] is the axial length of the Field-shaper, that need to be about 1 wind longer then the coil used,

[a] is the work-zone radius,

[b] is the work-zone width, and

[α] is the angle of focusing.

Document: Pulsar, “Basic principles of fieldshaper design

# Comparison of steel Fieldshaper at 10 µs with

$$C = \frac{B}{b + \frac{a\sin(\alpha)}{1-\cos(\alpha)}}$$

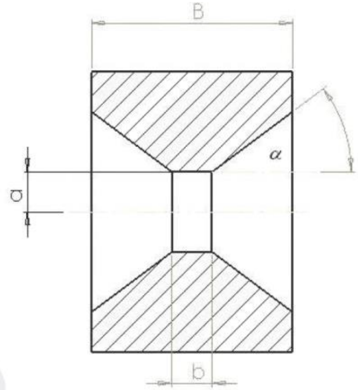


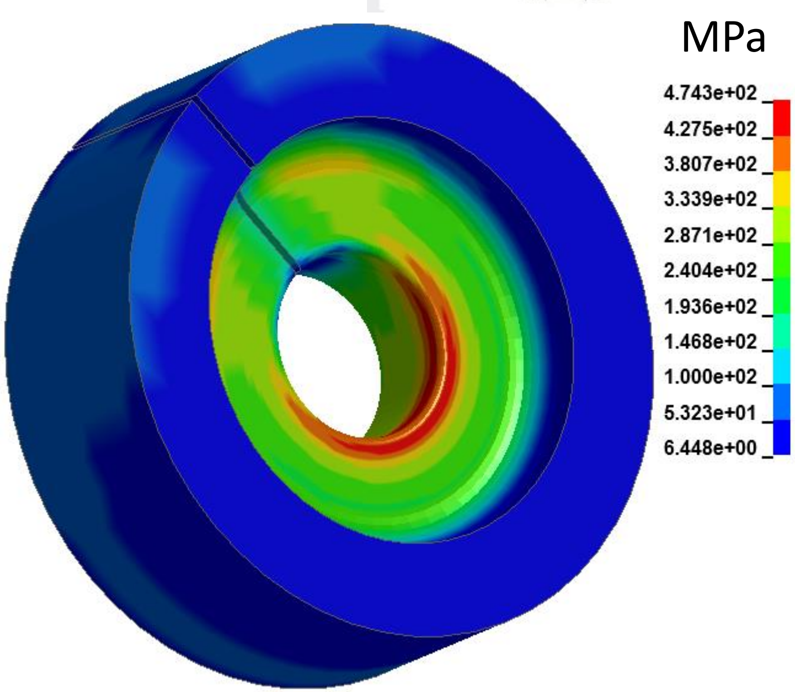


80 mm Fieldshaper

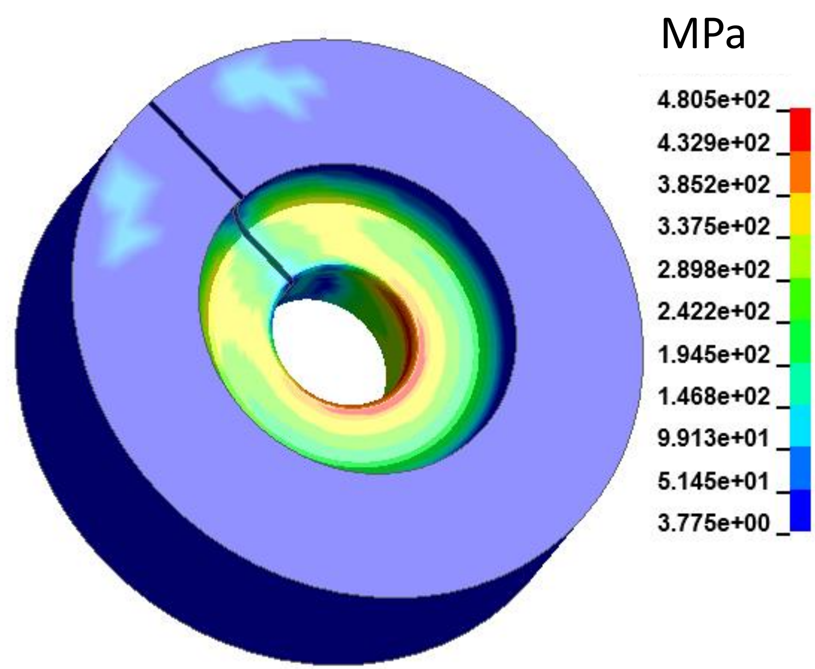


100 mm Fieldshaper

Document: Pulsar, “Basic principles of fieldshaper design

# Comparison of fieldshaper made of copper alloy with 89% IACS

$$C = \frac{B}{b + \frac{a\sin(\alpha)}{1-\cos(\alpha)}}$$

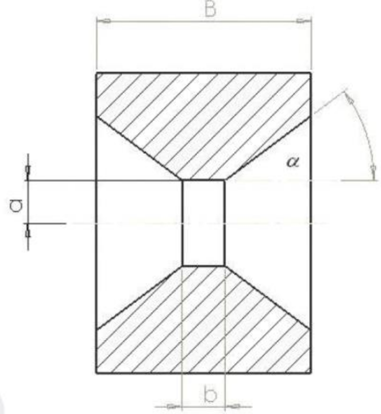


At 10 μs

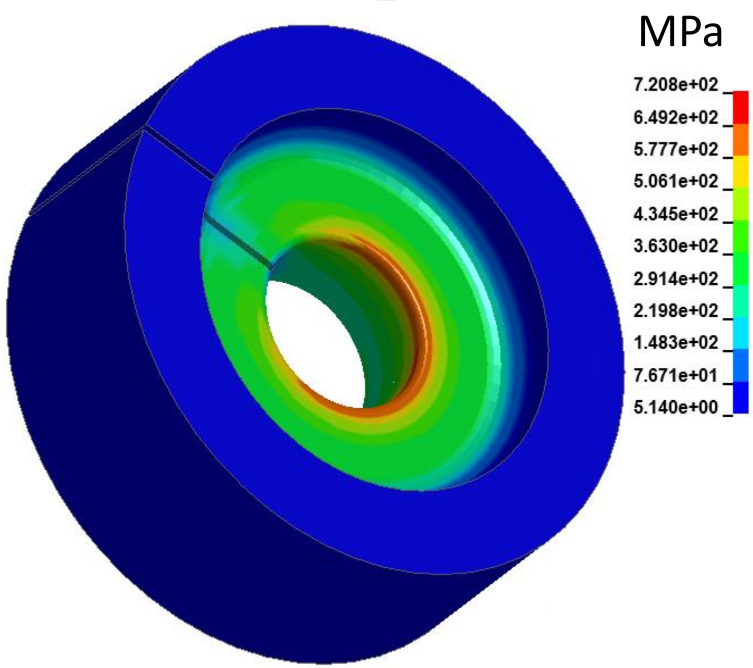


80 mm Fieldshaper

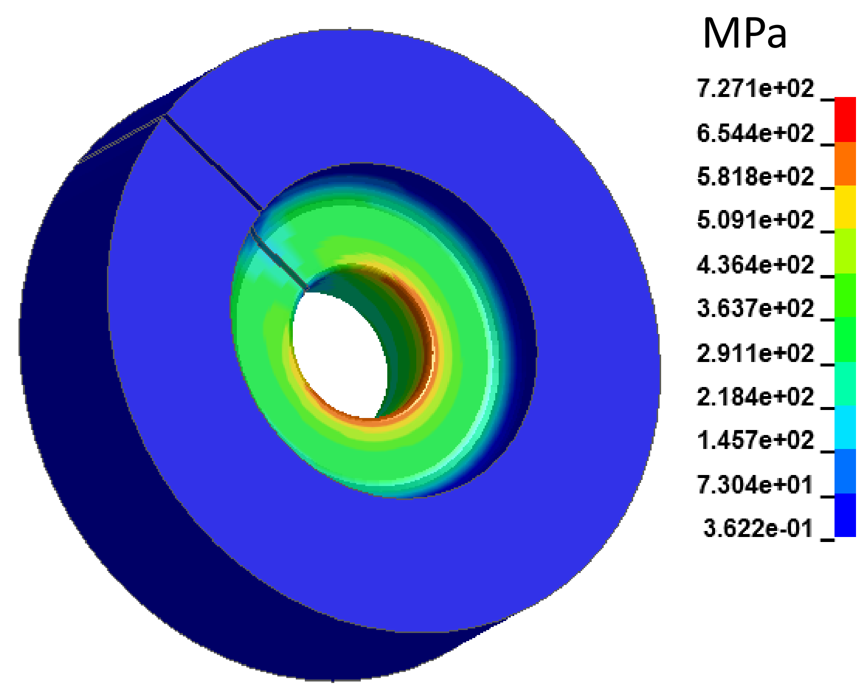


100 mm Fieldshaper

Document: Pulsar, “Basic principles of fieldshaper design

# Comparison of Lorentz force against time at various locations

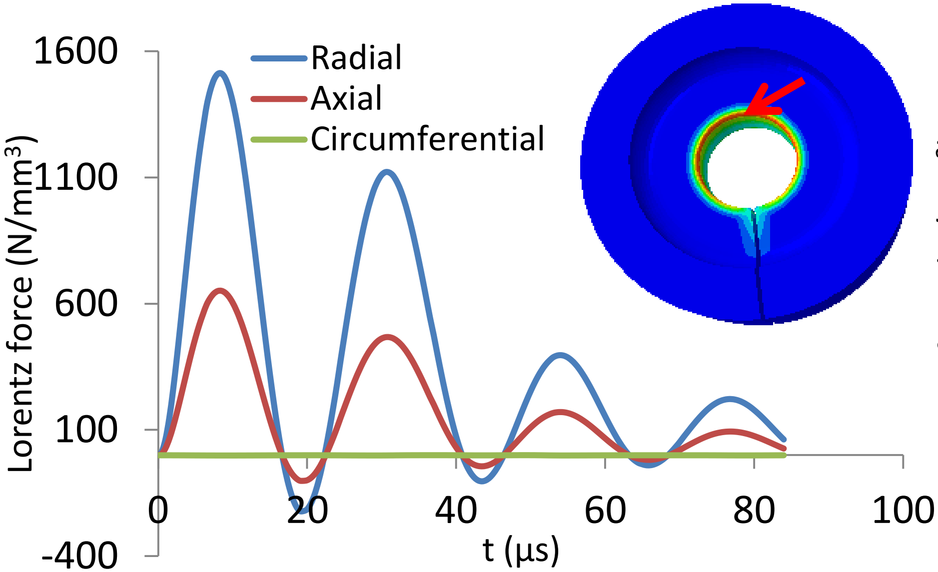


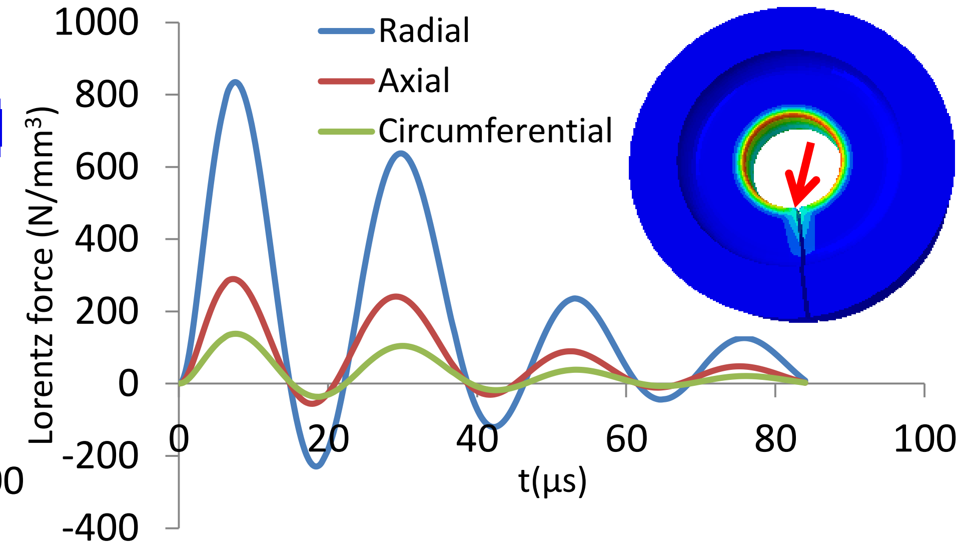


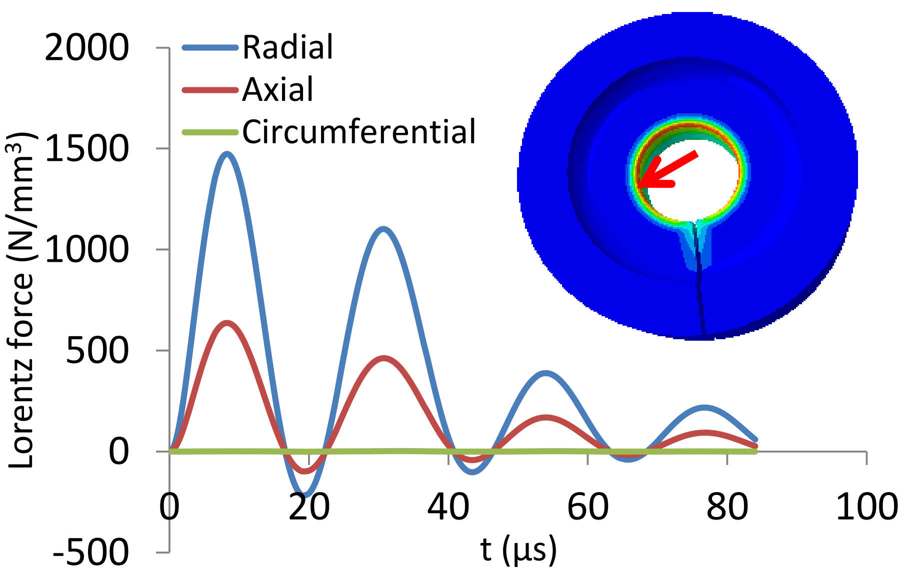


- On a copper alloy with 46% IACS
- Fieldshaper with 80 mm diameter

# Comparison of Lorentz force in space

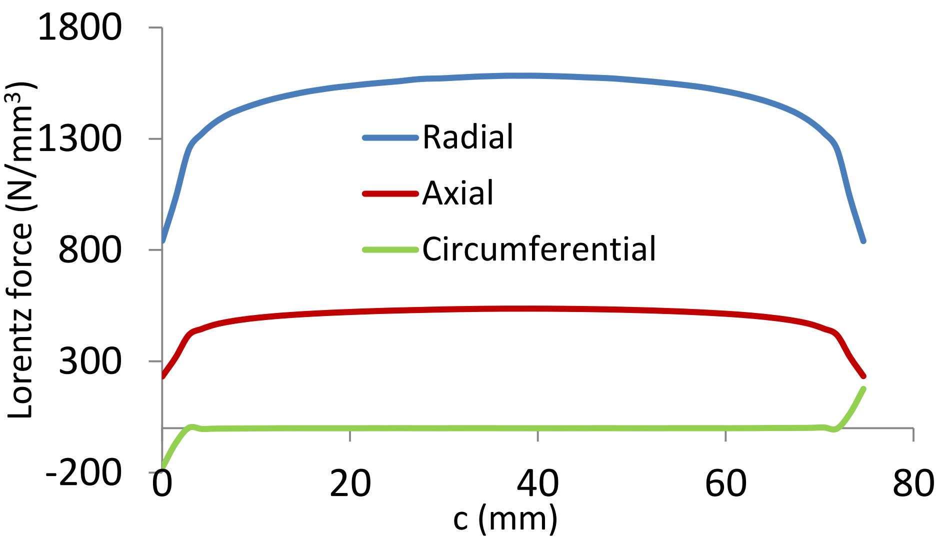


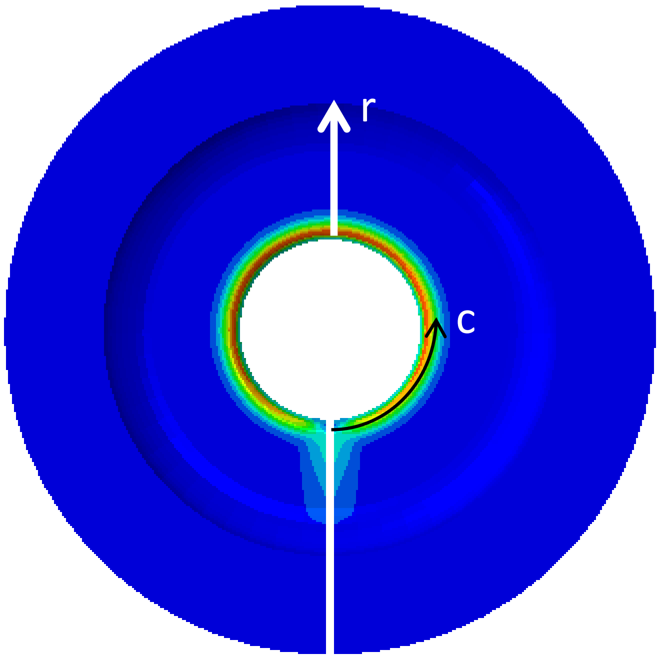


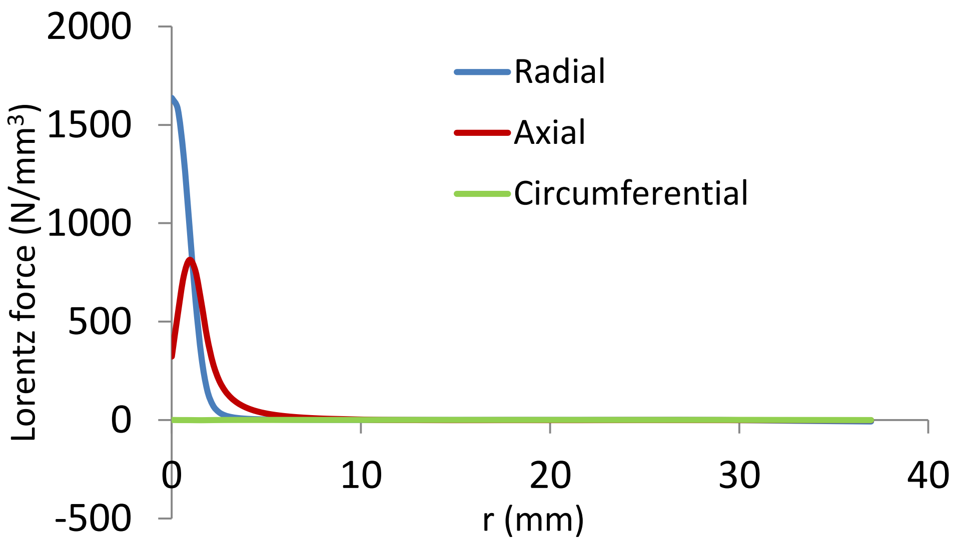


- On a copper alloy with 46% IACS
- Fieldshaper with 80 mm diameter

# Stress development over the time period, 46% IACS

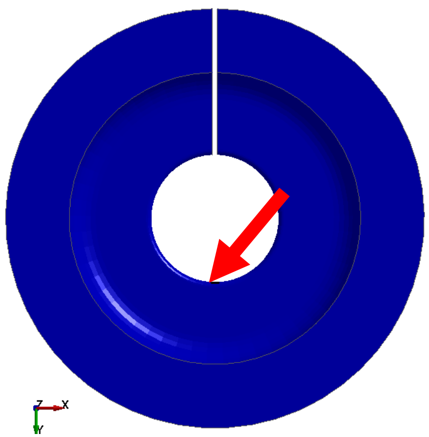

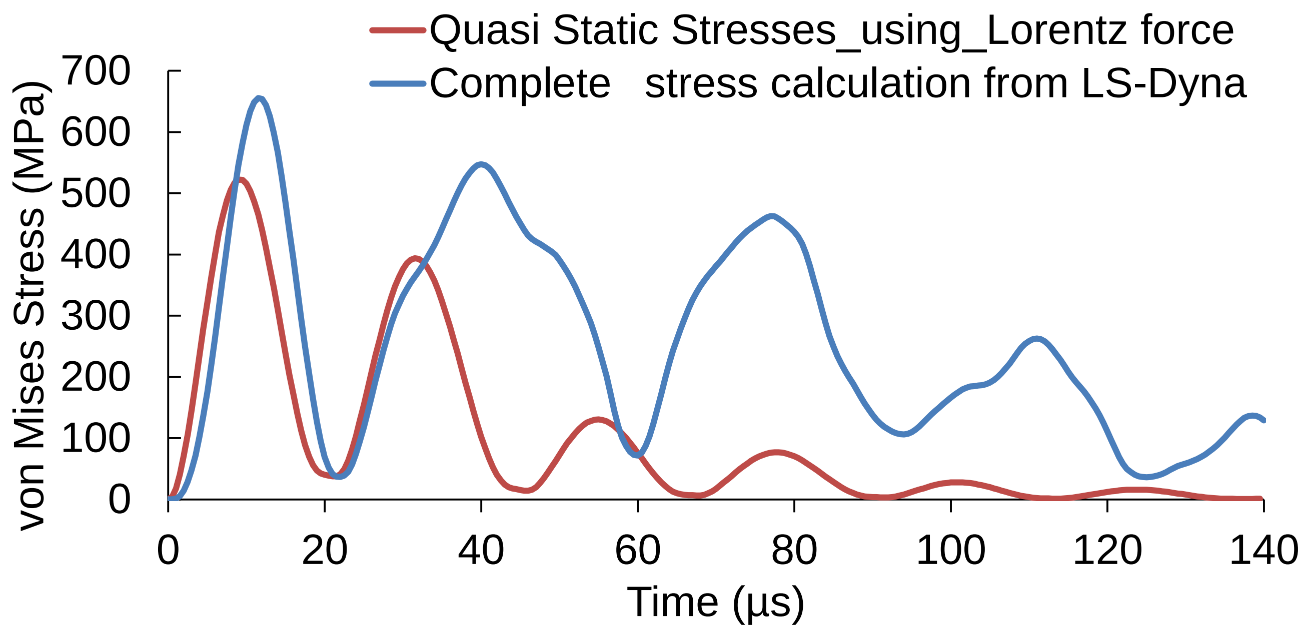


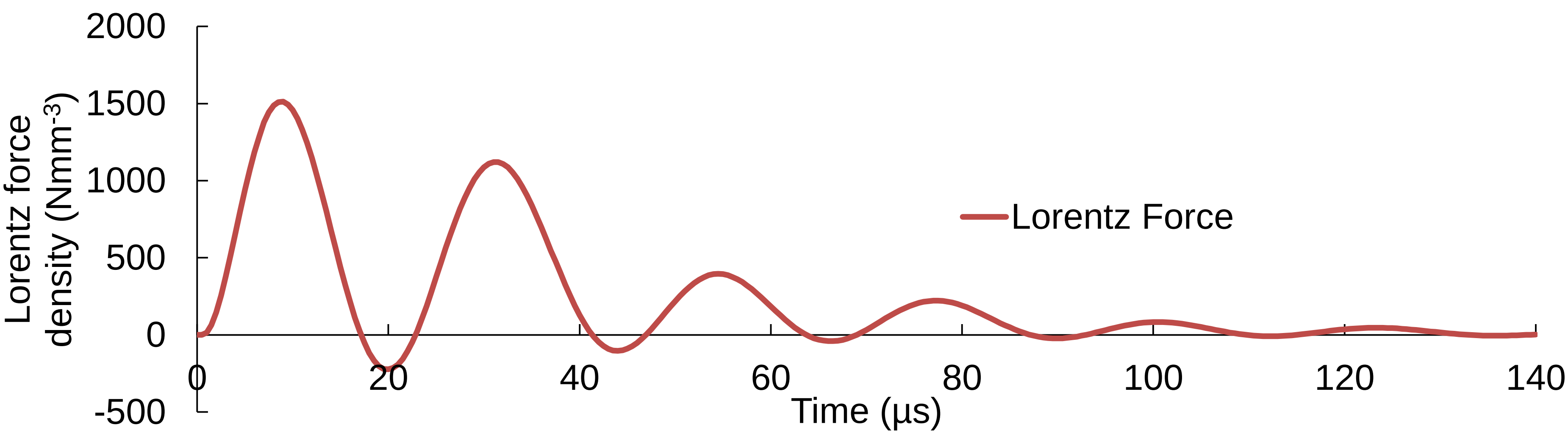

# Fatigue analysis of fieldshaper

The quasi static stress which is calculated using Lorentz force obtained from LS-Dyna

Electro magnetic calculation from LS-Dyna → Stress from quasi-static calculation → Fatigue calculation in FE-safe

Comparison of different number of current cycles, using von Mises - Goodman algorithm

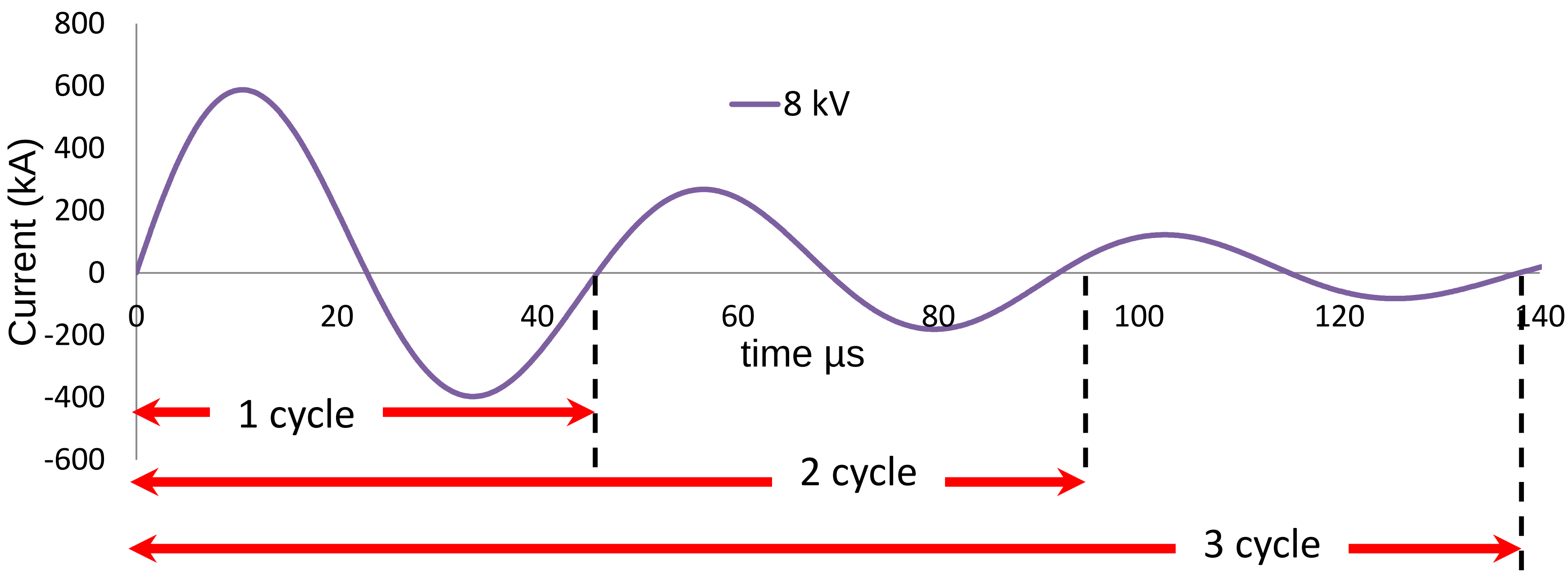

# Fatigue results of fieldshaper

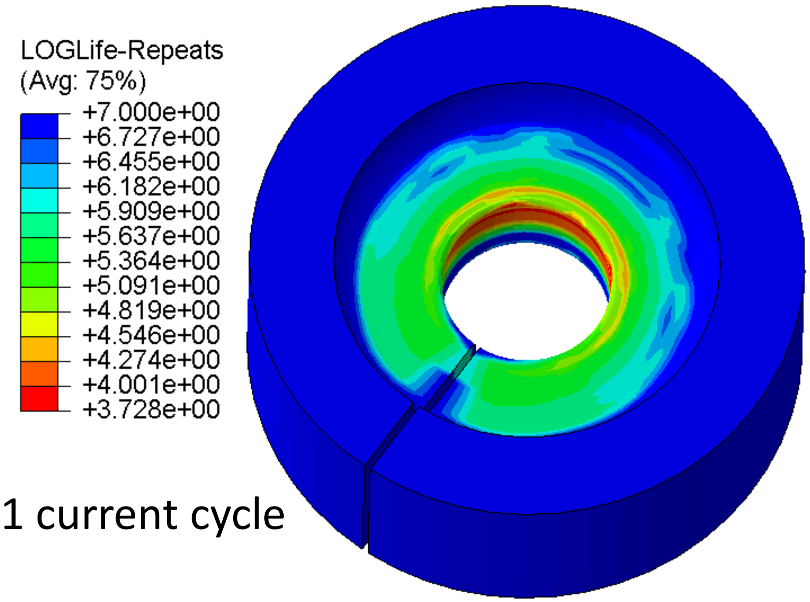


1 current cycle

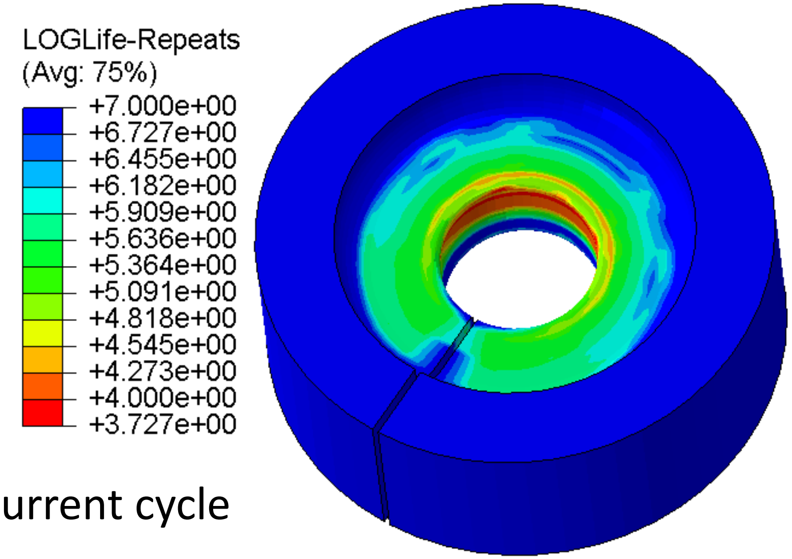


2 current cycle

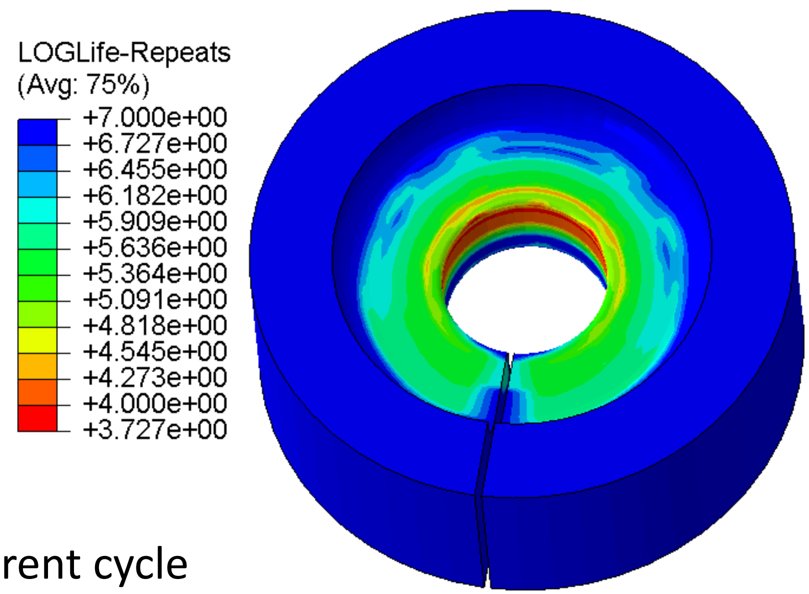


3 current cycle

The shortest life was predicted as 3804.284 life cycles with the quasi-static loading condition for all three cases

# Experimental and numerical interfacial characterisation

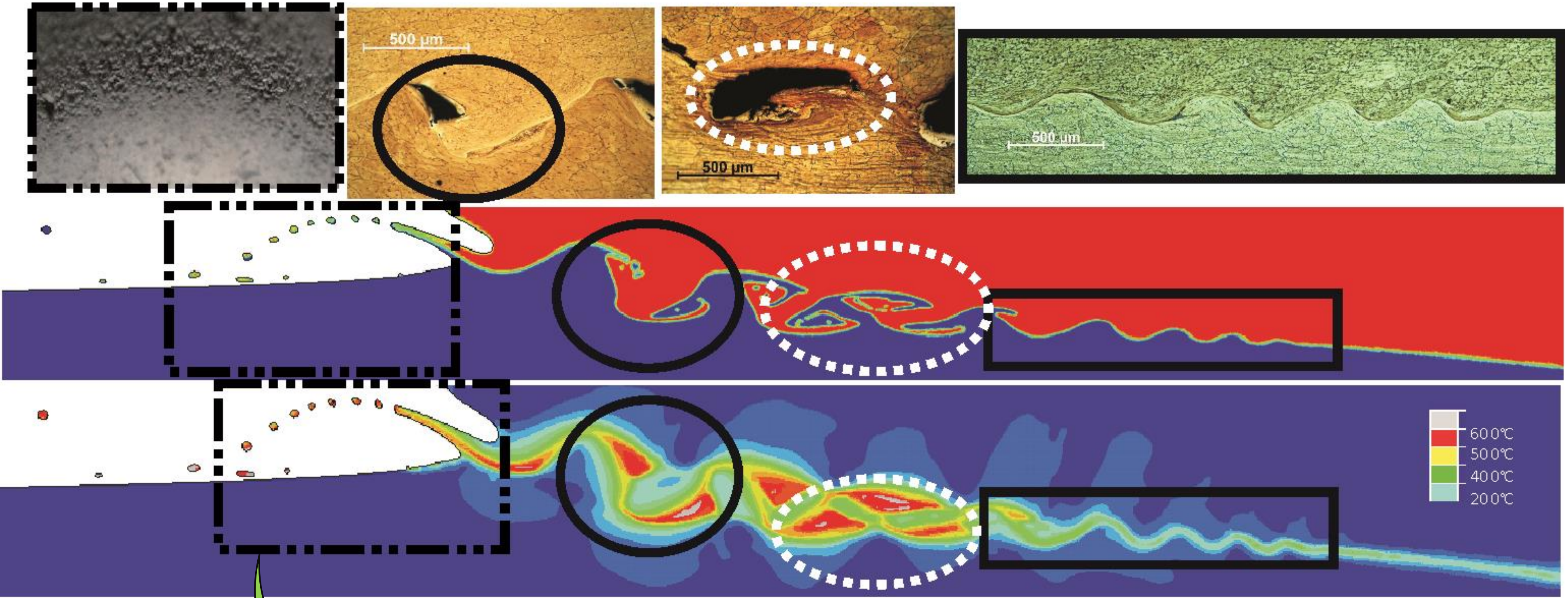


Particle Ejection Phenomenon

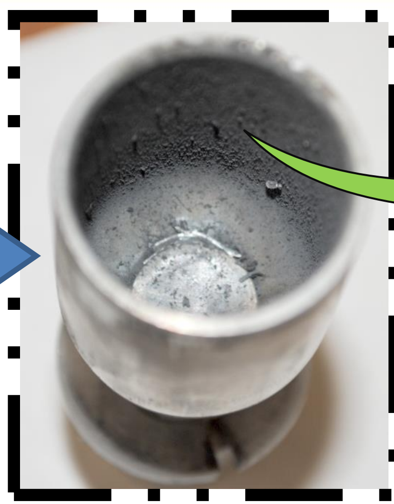

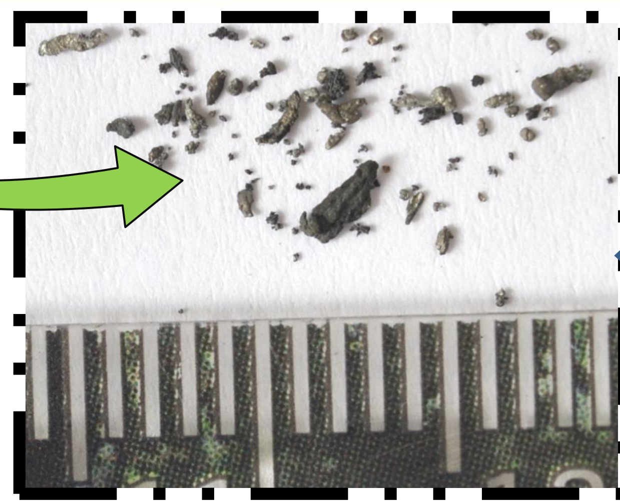

Agglomerates from Al/Al welds

# Conclusions

- The high speed multi-physics nature of the process, requires sophisticated numerical models
- Numerical models were developed for MPF/MPW to predict the stresses on the inductor parts
- Stresses on helix coil, flat coil and fieldshaper geometries are presented
- The stress development in fieldshaper shows an influence  due to the dynamic effect
- Cyclic loading and fatigue damage on the fieldshaper is also investigated

[MPF/MPW: Magnetic Pulse Forming / Magnetic Pulse Welding]

# Acknowledgement

We would like to thank the “Région Picardie” and “Le Fonds européen de développement régional (FEDER)” for their financial support

UNION EUROPEENNE

L’allocation post-doctorale relative au projet COILTIM est cofinancée dans le cadre du Fonds européen de développement économique et régional (FEDER) 2014/2020.

# Stress analysis on the inductor parts during electromagnetic pulse forming and welding processes using numerical simulations

Thank you for your attention

L'allocation post-doctorale relative au projet COILTIM est cofinancée dans le cadre du Fonds européen de développement économique et régional (FEDER) 2014/2020.